

Provenance analysis of the Voirons Flysch (Gurnigel nappe, Haute-Savoie, France): stratigraphic and palaeogeographic implications

Jérémie Ragusa¹, Pascal Kindler¹, Branimir Segvic², Lina Maria Ospina-Ostios³

¹ University of Geneva, Department of Earth Sciences, 13, Rue des Maraîchers, CH-1205 Geneva, Switzerland
Contact: Jérémie Ragusa (jeremy.ragusa@unige.ch)

² Texas Tech University, Department of Geosciences, 1200 Memorial Circle, Lubbock, TX 79409, USA

³ Universidad del Valle, Escuela de Ingeniería Civil y Geomática, Cali, Colombia

International Journal of Earth Sciences, 106(8):2619–2651, doi: [10.1007/s00531-017-1474-9](https://doi.org/10.1007/s00531-017-1474-9)

Abstract

The Chablais Prealps (Haute-Savoie, France) represent a well-preserved accretionary wedge of the Western Alpine Tethys. They comprise a stack of sedimentary nappes related to palaeogeographic realms ranging from the Ultrahelvetic to the Southern Penninic. The provenance analysis is based on the Gazzi-Dickinson method, and on QEMSCAN® for heavy-minerals. The Quartzose petrofacies is the most important of the two sources, and supplied three of the four formations of the Voirons Flysch. It is similar to the sources that fed the other flyschs from the Gurnigel nappe. It is characterised by a mature, quartz-rich assemblage and a heavy mineral population dominated by apatite and the zircon-tourmaline-rutile mineral group. These observations suggest a Clastic wedge provenance. The Feldspathic petrofacies is derived from a feldspar-rich source associated with metamorphic clasts and a heavy mineral population dominated by garnet. This provenance characterises only one formation of the Voirons Flysch, and is related to the Axial Belt provenance.

This provenance analysis shows that the Middle Eocene to Early Oligocene Voirons Flysch was fed by two sources, in contrast to the other flyschs of the Gurnigel nappe, and further suggests that this flysch was not deposited in the Piemont Ocean but in the Valais domain. Based on the results and comparative provenance analysis with the other flyschs of the Gurnigel nappe, we propose a generic feeding model which involves the Sesia-Dent Blanche nappe, the sedimentary nappes incorporated in the accretionary prism, and probably the Briançonnais basement.

Keywords

Gurnigel nappe, Chablais Prealps, Voirons Flysch, Provenance, QEMSCAN®, Heavy-mineral, Valais domain

1 Introduction

The Alps are one of the most studied mountain chains in the world, and recent palaeogeographic reconstitutions have shed light on the distribution of tectonic units and the timing of their incorporation into the orogenic belt (Schmid et al., 1996, 2004 ; Stampfli and Borel, 2002 ; Stampfli et al., 2002 ; Handy et al., 2010). The palaeogeographic reconstructions of sedimentary covers are partly based on age data, with the youngest age indicating the end of sedimentation in the basin and its subsequent incorporation into the accretionary prism (Stampfli et al., 2002). Most of these youngest and highest sedimentary successions essentially consist of flysch deposits. Provenance studies on the extrabasinal detrital fraction of these flyschs are highly used for palaeogeographic reconstructions. These studies normally rely on petrographic and mineralogical analogies with hypothesised source materials (von Eynatten and Gaupp, 1999 ; Beltrán-Triviño et al., 2013) which help to establish the sedimentary flux and to estimate the successive exhumation of the detrital sources through time (Trautwein et al., 2001). The techniques of provenance analysis have markedly improved in the last decades with the refinement of the tectonic settings of the source rocks (Dickinson and Suczek, 1979 ; Dickinson et al., 1983 ; Dickinson, 1985), the development of statistical tools to constrain the sediment source (Garzanti et al., 2004 ; Garzanti and Andò, 2007 ; Garzanti et al., 2007, 2010) and the geochemistry of single grains (von Eynatten and Dunkl, 2012).

In the Alps, many sedimentary cover nappes are separated from their crystalline basement which complicates the identification of their original palaeogeographic location. In particular, the palaeo-depositional realm of the Cretaceous to Eocene Gurnigel nappe, a flysch nappe now exposed in the Swiss and French Prealps (Fig. 1), is most controversial, as it has been successively placed in the Ultrahelvetic domain (Lombard, 1940 ; Hsü, 1960 ; Trümper, 1960 ; Hubert, 1967 ; Hsü and Schlanger, 1971), along the southern margin of the

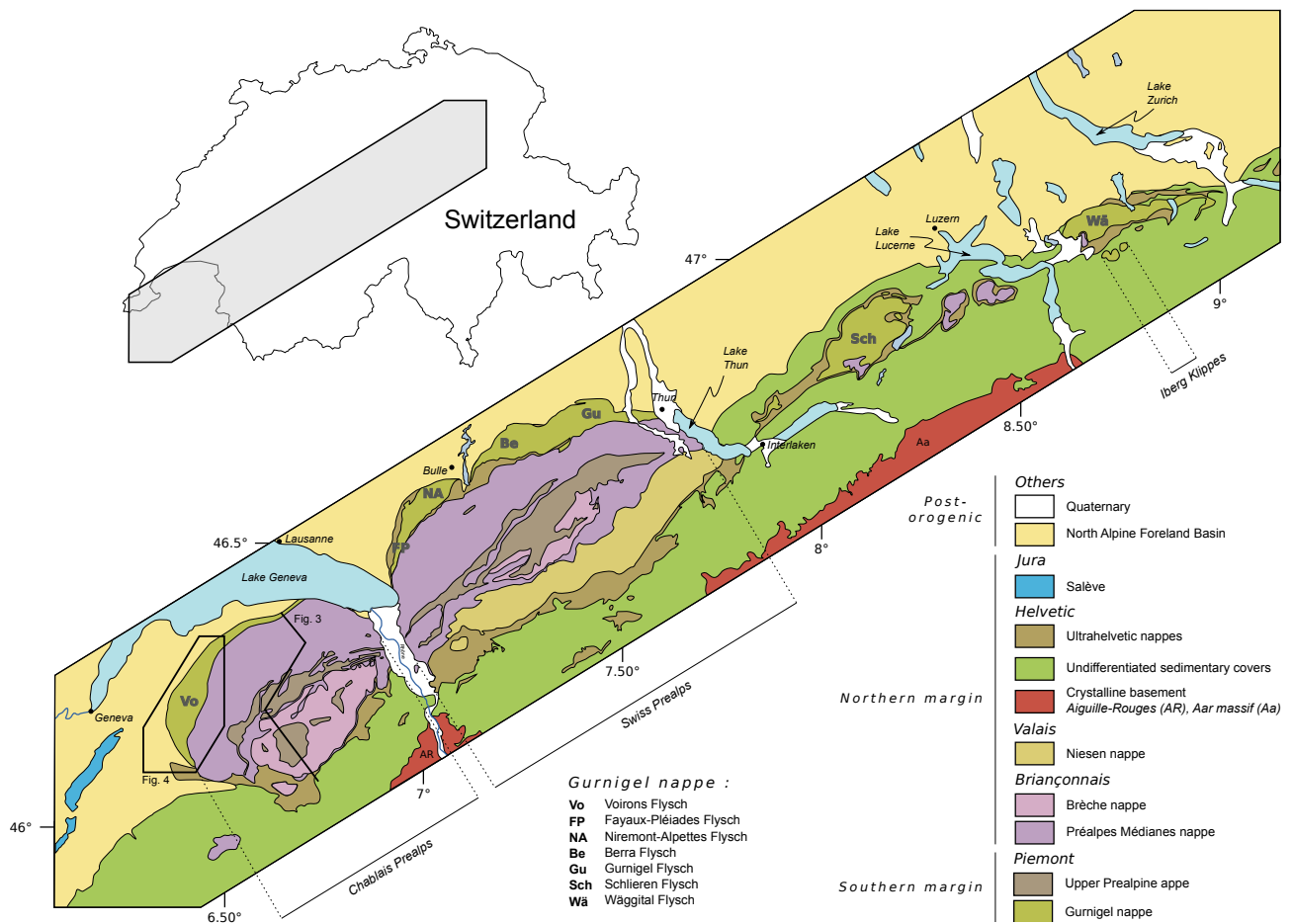


Figure 1: Tectonic map of the Chablais and Swiss Prealps (SwissTopo, 2008, modified) with the location of the different flyschs of the Gurnigel nappe. The black box indicates the studied area described in Fig. 4.

Piemont Ocean (Caron, 1976 ; Winkler, 1983, 1984), and, more recently, in the Valais trough (Trümpy, 2006 ; Ospina-Ostios et al., 2013 ; Ragusa, 2015) (Fig. 2).

The goal of this study is to analyse the framework composition and heavy-mineral assemblage of the Middle Eocene to Early Oligocene Voirons Flysch which corresponds to the western extension of the Gurnigel nappe in France (Fig. 1). These new data provide unsuspected information on the source regions of this flysch, and help in refining its stratigraphical context. Data are further compared with similar results from other parts of the Gurnigel nappe and from various Prealps flyschs (Figs. 1 and 2; Caron et al., 1989), and finally are used to formulate an original palaeogeographic model for the Voirons Flysch.

2 Geological background

The Prealps form moderately elevated reliefs (ca. 2 000 m) between Lake Geneva and Lake Zurich (Fig. 1). They include, in particular, the Chablais massif, south of Lake Geneva, and the Swiss Prealps, between Lake Geneva and Lake Thun. These reliefs encompass a stack of sedimentary cover nappes detached from their respective basement during the Alpine subduction, and follow a thin-skinned, in-sequence thrusting (Figs. 1 and 3; Mosar, 1991 ; Wissing and Pfiffner, 2002). They represent the former sedimentary accretionary to orogenic prism of the Alpine Tethys in this part of the Western Alps (Stampfli et al., 1998 ; Handy et al., 2010). Nowadays, they overlie the Helvetic nappes to the SE and the North Alpine Foreland Basin (NAFB) to the NW (Fig. 1). Due to the NW translation of both of these units, the frontal edge of the Prealps includes tectonic slices from the Helvetic nappes (e.g. the Subalpine Flysch) and from the subsequent filling-up of the NAFB (e.g. the Subalpine Molasse). These units are separated from the Prealps nappes by the Intraprealpine mélange (Fig. 4; Jeanbourquin et al., 1992).

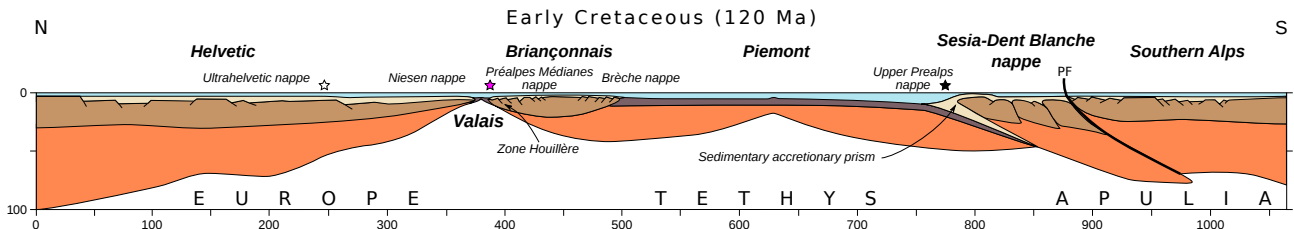


Figure 2: Simplified palinspastic model from Stampfli et al. (1998, modified) with the original location of the Prealps nappes. Stars represent the successive paleogeographic attribution of the Gurnige nappe: Ultrahelvetic realm (white), South Penninic (black) and Valais domain (purple).

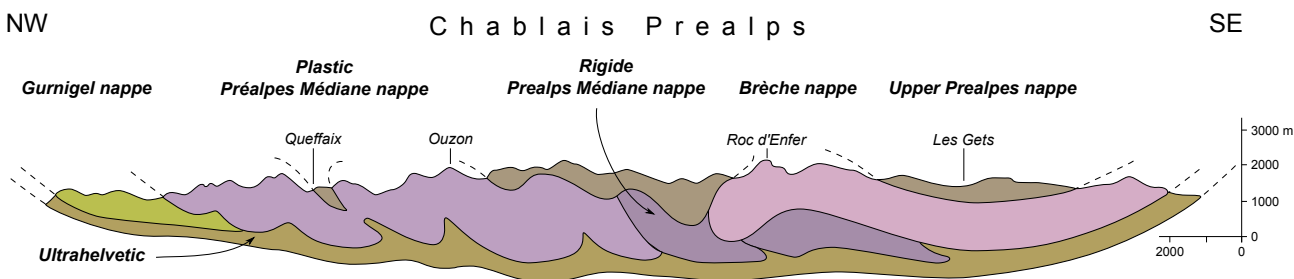


Figure 3: Cross-section of the Chablais Prealps from Caron (1972, modified).

The Gurnigel nappe is one of the lowermost nappes of the Prealps, and is exposed along their NW edge (Figs. 1 and 3). It comprises several flysch units generally interpreted as gravity-flow deposits: Voirons (Lombard, 1940; Ospina-Ostios et al., 2013; Ragusa, 2015), Fayaux (Van Stijvenberg et al., 1976; Weidmann et al., 1976; Jan du Chêne, 1977; Weidmann, 1985), Niremont (Morel, 1980; Ambrosetti, 2005), Berra (Tercier, 1928), Gurnigel (Van Stijvenberg, 1979), Schlieren (Winkler, 1983, 1984, 1993) and Wägital (Winkler et al., 1985a). These different flysch successions share similar lithostratigraphic characteristics. Indeed, previous mineralogical studies in the Gurnigel (Van Stijvenberg, 1979), Schlieren (Winkler, 1983, 1984) and Wägital (Winkler et al., 1985a) flyschs show that constituent rocks are characterised by a quartz-feldspar dominated modal composition with subordinate lithics and a heavy-mineral population dominated by zircon-tourmaline-rutile (ZTR) and garnet (Wildi, 1985). The presence of peculiar agglutinated foraminifers (Rhabdamina fauna; Brouwner, 1965; Weidmann, 1967; Van Stijvenberg et al., 1976; Ujetz, 1996), the nature of bioturbations (Crimes et al., 1981), and the sedimentological features (Kuenen and Carozzi, 1953), all suggest a deep-marine sedimentary environment for these successions. Early biostratigraphic studies based on calcareous nannofossils, dinoflagellates and, more rarely, on planktonic foraminifers indicated a Late Maastrichtian to Lutetian age for all flysch units of the Gurnigel nappe (Rigassi, 1958; Kuhn, 1972; Jan du Chêne et al., 1975; Jan du Chêne, 1977; Van Stijvenberg, 1979; Winkler, 1983, 1984; Winkler et al., 1990; de Kaenel et al., 1989). Such an age range is also supported by the occurrence of bentonite layers dated from the Paleocene in the lower part of the Schlieren Flysch (Winkler et al., 1985b; Koch et al., 2015), and possibly related to the North Atlantic events (Egger et al., 2005). However, planktonic foraminifers of Middle to Late Eocene/Early Oligocene age have recently been retrieved from the Voirons Flysch (Ujetz, 1996; Ospina-Ostios et al., 2013).

For long, the flysch units outcropping along the NW edge of the Prealps were thought to originate from the Ultrahelvetic realm (e.g. Tercier, 1928; Lombard, 1940; Fig. 2), but several authors had already noticed the petrographical resemblance of some conglomerate clasts found in these units (e.g. pink granite fragments) with several rock bodies exposed in the Southern Alps (Sarasin, 1894; Pilloud, 1936; Lombard, 1940; Cogulu, 1961) such as the Bernina nappe, Canavese zone, Err-Albula granite, Falknis nappe, etc. Later, based on petrographic and biostratigraphic data, Caron (1976) regrouped all these flyschs in a new tectonic unit, the Gurnigel nappe, which he correlated with the Sarine nappe (Upper Prealps nappe, Fig. 2) of South-Penninic origin. Detrital grains were thought to originate from the Austroalpine domain (Winkler, 1983; Caron et al., 1989). The peculiar structural position of the Gurnigel nappe at the base of the Prealps nappe stack was then explained by the overthrusting of the Upper Prealps beyond the front of the Préalpes Médianes nappe, followed by out-of-sequence thrusting of the latter (Mosar, 1991; Wissing and Pfiffner, 2002). However, recent structural

data from the Iberg Klippe (Trümpy, 2006) and the younger age found by Ujetz (1996) and Ospina-Ostios et al. (2013) now suggest that the Gurnigel flyschs could have been deposited in the Valais Ocean (Fig. 2), which would considerably simplify the kinematics of the Prealps.

3 Study area

The Voirons Massif, which comprises the western portion of the Gurnigel nappe, is located in the Chablais Prealps, at about 20 km from Geneva (Figs. 1 and 3). It includes a series of smoothed hilltops, which are, in decreasing order of altitude, the Voirons (1480 m), the Grande Combe (1293 m), the Mont Vouan (978 m) and the Allinges Hills (754 m). The latter broadly constitute the eastern limit of the massif. The Voirons Massif is essentially made of flysch deposits (Lombard, 1940 ; Jan du Chêne et al., 1975 ; Van Stuijvenberg, 1980), whose stratigraphy has recently been revised (Ragusa, 2015; Fig. 4). Accordingly, it now comprises four lithostratigraphic units:

1. The Voirons Sandstone Formation forms the crest and the eastern flank of the Voirons ridge (Fig. 4). It is a thick (200 to 300 m), sandstone-rich succession with variable amounts of intercalated marls (Figs. 5a and 5b). The base of the unit is marked by a marly succession with calcarenous beds (Fig. 5a) similar to the Hellstät Formation of the Gurnigel Flysch (Tercier, 1928 ; Caron et al., 1980, 1989). Some m-thick conglomeratic layers are exposed along the Voirons crest. Described as “local deposits” by Lombard (1940), they include the pink granite lithoclasts (Fig. 6a) typical of the flyschs from the Gurnigel nappe (Caron, 1976). The Voirons Sandstone Fm. presents a large range of sedimentary deposits from channel to lobe settings (Ragusa, 2015). Deposition is constrained between the Middle Eocene and the Early Oligocene (planktonic foraminiferal zones P12 to P19, Ospina-Ostios et al., 2013). The contact with the overlying Vouan Conglomerate Fm. is transitional (Ragusa, 2015).
2. The Vouan Conglomerate Formation is exposed along the eastern flank of the Voirons ridge, and forms the neighbouring Mont Vouan (Fig. 4). It is a homogeneous stack (300 - 400 m thick) of coarse pebbly sandstones to matrix-supported conglomerates that are frequently amalgamated (Fig. 5c). They are mostly devoid of marly intervals, and include black sandstone and conglomerate lithoclasts of Paleozoic age (Fig. 6b). Pebbles and cobbles are also randomly distributed in sandy layers. Lateral variation and large scours (Frébourg, 2006) characterise the Vouan Conglomerate Fm. which is restrained to channel depositional settings (Ragusa, 2015). The scarce biostratigraphic data from this unit (Frébourg, 2006 ; Ospina-Ostios et al., 2013) suggest a Late Eocene – Early Oligocene age (planktonic foraminiferal zones P15 to P20). The contact with the Boëge Marl Fm. is sharp and does not present any tectonic deformation (Ragusa, 2015).
3. The Boëge Marl Formation (synonymous: Saxel Marl Fm.) was defined by Van Stuijvenberg and Jan du Chêne (1980), and comprises the Ludran Hills and the Grande Combe. It is one thick (> 1000m), predominantly marly succession, interspersed by cm-thick, sandstone-rich layers. The base is characterised by some dm-thick conglomeratic layers. The sandstone beds show frequent ripples and upper-plane bedding (Fig. 5d). The formation is affected by several tectonic folds and thrusts (Coppo, 1999 ; Ragusa, 2015). This unit is interpreted as lobe or continental-slope deposits (Winkler, 1984). The Boëge Marl Fm. shows a tectonic contact with the Préalpes Médianes nappe in the southern part of the studied area and a stratigraphic (?) contact with the overlying Bruant Sandstone Fm. in the Grande Combe area. Indeed, the progressive upward thickening of sandstone beds suggests a transitional contact. The Boëge Marl Fm. is of late Middle Eocene to Early Oligocene age (Ospina-Ostios et al., 2013; planktonic foraminiferal zones P13 to P20).
4. The Bruant Sandstone Formation (Ragusa, 2015) consists of dm-thick, sandy beds interspersed by cm-thick, marly intervals. No conglomeratic intervals have been found in this formation, but its upper reaches comprise some microconglomerate layers. Its upper limit corresponds to the tectonic contact with the Préalpes Médianes nappe. From a petrographic viewpoint, the Bruant Sandstone Fm. is comparable to the Voirons Sandstone Fm., and is interpreted as channel to lobe deposits (Ragusa, 2015). No biostratigraphic data have so far been retrieved from this unit. The formation thickness is estimated at about 1000 m. Up to now, this unit was incorrectly interpreted as a sedimentary mélange (Kerrien et al., 1998) because of the pronounced (tectonic) deformation near the contact with the Préalpes Médianes nappe.

4 Methods

4.1 Sampling

Total amount of 278 sandstone samples was collected in about fifty outcrops of the Voirons Flysch. An additional exposure, the Fenalet quarry (Fig. 5f), to the East of the Allinges Hills, was also investigated, although it is generally attributed to the Ultrahelvetic because of its structural position and age (Gagnebin, 1944 ; Badoux, 1962, 1965, 1996). The Fayaux (Fig. 5g; Van Stuijvenberg et al., 1976) and the Zollhaus quarries (Fig. 5h; Bouma, 1962 ; Crimes et al., 1981), that comprise respectively the Fayaux-Pléiades and the Berra flyschs, were also sampled for comparative purposes. Geographic location of the outcrops, stratigraphic logs and datasets are available on the GitHub page of the first author (<https://github.com/jragusa/>).

4.2 Thin-section modal mineralogy

Counting was performed according to the Gazzi-Dickinson method (Dickinson and Suczek, 1979 ; Ingersoll and Suczek, 1979 ; Dickinson, 1985). Grains were organised following the Zuffa classification (Zuffa, 1980). 300 extrabasinal grains was counted per thin section using the ribbon method of Van der Plas (1962). Feldspar minerals were stained following the procedure developed by Norman (1974) and advices from Prof. Wilfried Winkler (ETH-Zürich). Using this technique, albite remains colourless but, in contrast to quartz grains, it is etched along the cleavage planes. Grains included in rock fragments (quartz, feldspars and micas) were counted separately (Critelli et al., 2007 ; Stefani et al., 2007 ; Das Gupta and Pickering, 2008) and described according to the nomenclature of Weltje (2002) (–rv: volcanic rock, –rm: metamorphic rock, –rg: plutonic rock). Sand-size quartz and feldspars from igneous rock fragments are reported in their respective QAP ternary diagram (Quartz – Alkali feldspar – Plagioclase). By convention, we distinguished lithic fragments (i.e. polycrystalline grains with internal grain-size less than 63 µm) from rock fragments (internal grain-size coarser than 63 µm). Metamorphic lithic and rock fragments were determined following the colour guide of Garzanti and Vezzoli (2003). They are distributed between the low- (Rm1+), intermediate- (Rm3+) and high-metamorphic (Rm5+) grades, and described using the MI index (Metamorphic Index: Garzanti et al., 2004, 2010). Considering the sand-size limit, metamorphic grains of grade five were counted as rock fragments (Rm5). The status of mudstone and wackestone lithoclasts (Figs. 6c and 6d) is still questionable as there is no undisputable evidence for an extrabasinal origin (Zuffa, 1980). They can be inherited from a sedimentary cover (extrabasinal origin) or reworked from a platform (intrabasinal origin; Critelli et al., 2007). In addition, the incorporation of calcareous grains in the counting is debated (Dickinson and Suczek, 1979 ; Mack, 1984). Calcareous grains are very sensitive to weathering and a small amount of terrestrial calcareous grains reaches marine basins (Arribas et al., 2000 ; Picard and McBride, 2007). Considering that inclusion of detrital carbonate grains confers consistent provenance interpretation in some cases (Mack, 1984), our results are presented without (continuous line) and with (dashed line) the micritic limestone clasts. In addition, grain counting includes also intrabasinal grains (authigenic and skeletal grains), cement and porosity.

Because formation boundaries are poorly defined in the Voirons Flysch (Van Stuijvenberg, 1980 ; Van Stuijvenberg and Jan du Chêne, 1980 ; Vial et al., 1989 ; Coppo, 1999), the framework composition of samples was sorted independently of stratigraphic affiliation using a cluster analysis (Ward method and Euclidean distance; Fig. 7). Only grain classes exceeding 10 % were selected (Qm, K, Lm, Qr, P, Ls, Lce, Qp, Lv and Lci; see Table ?? for description) to constrain the interpretation of the cluster tree, and limit the influence of minor grain classes. Each cluster defines a petrofacies which refers to similar compositional parameters (Dickinson and Rich, 1972).

4.3 QEMSCAN heavy mineral analyses

Heavy mineral were sampled from each petrofacies identified from the framework composition. They were extracted from fine- to medium-grained, well-preserved sandstones following Mange and Maurer (1992). The rocks were crushed and cement removed with acetic acid (10 %) in a hot bath (70°C). The 63–125 µm fraction of loose sediment was recovered by wet sieving. Dense minerals were separated using a liquor of sodium polytungstate (SPT) at $d = 2.90 \text{ g/cm}^3$, and recovered by freezing the bottom part of centrifugation tube. Heavy and light mineral fractions were then dried and weighted. Finally, the heavy mineral fraction was placed in moulds, consolidated with an epoxy resin, and subsequently polished to be analysed by an FEI QEMSCAN® Quanta 650F installed at the Department of Earth Sciences of the University of Geneva.

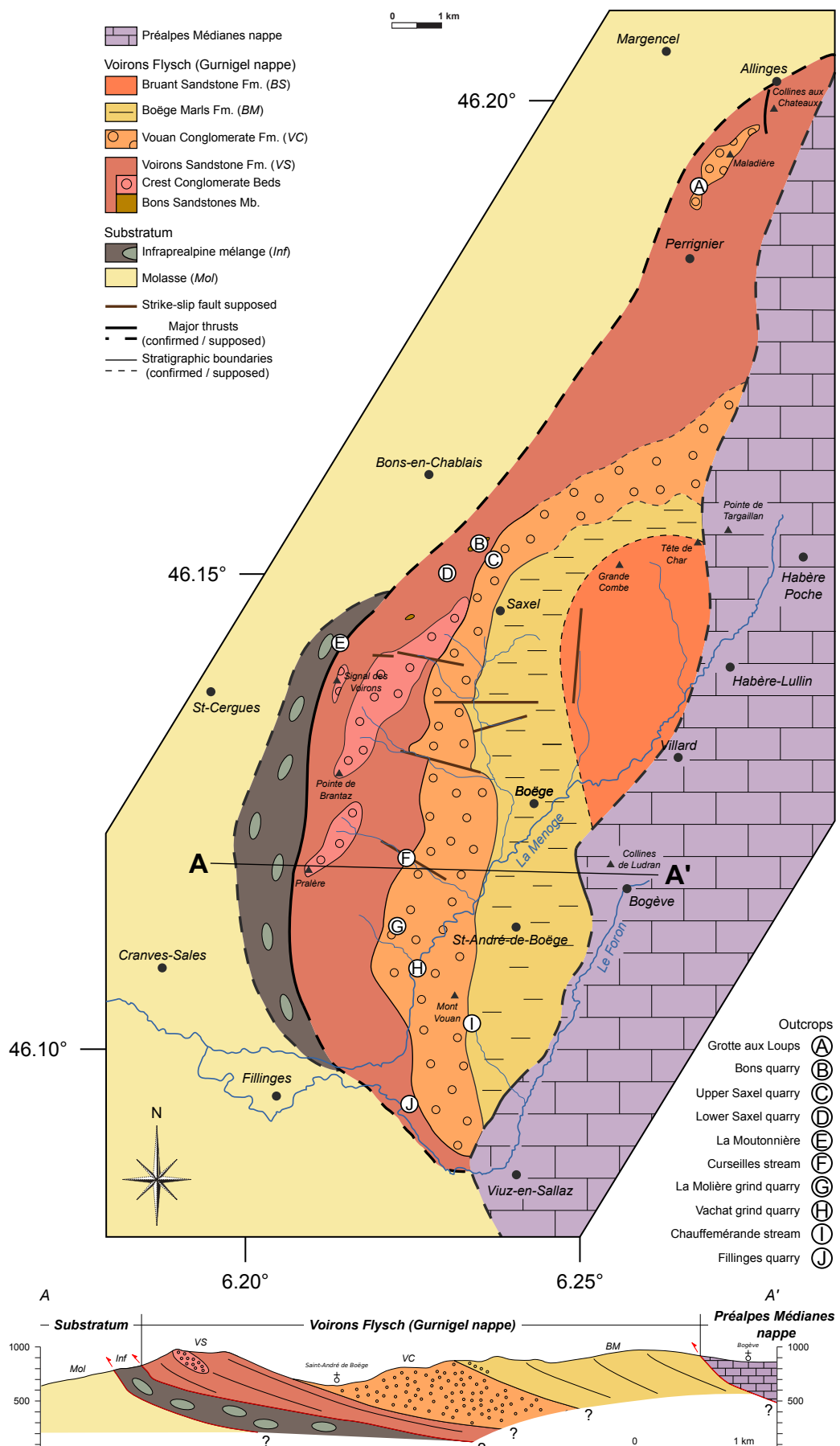


Figure 4: Tectonic map of the Voirons Flysch and associated cross section. The Bruant Sandstone Fm. is not represented in this section. The northern part of the Voirons Flysch is mostly covered by Quaternary deposits and does not outcrop. Beyond the Allinges Hills, outcrops of the Voirons Flysch are rare and the eastern limit is not well constrained.



Figure 5: Main studied outcrops: (a) the Bons quarry (VS), (b) the lower Saxel quarry (VS), (c) the Vachat millstone quarry (VC), (d) the Chauffemerande creek (BM), (e) The Grotte aux Loups (VC), (f) the Fenalet quarry (UH ?), (g) the Fayaux quarry (Fayaux-Pleiades Flysch) and (h) the Zollhaus quarry (Berra-Schwyberg Flysch). Location map is available in Figures 1 and 3.

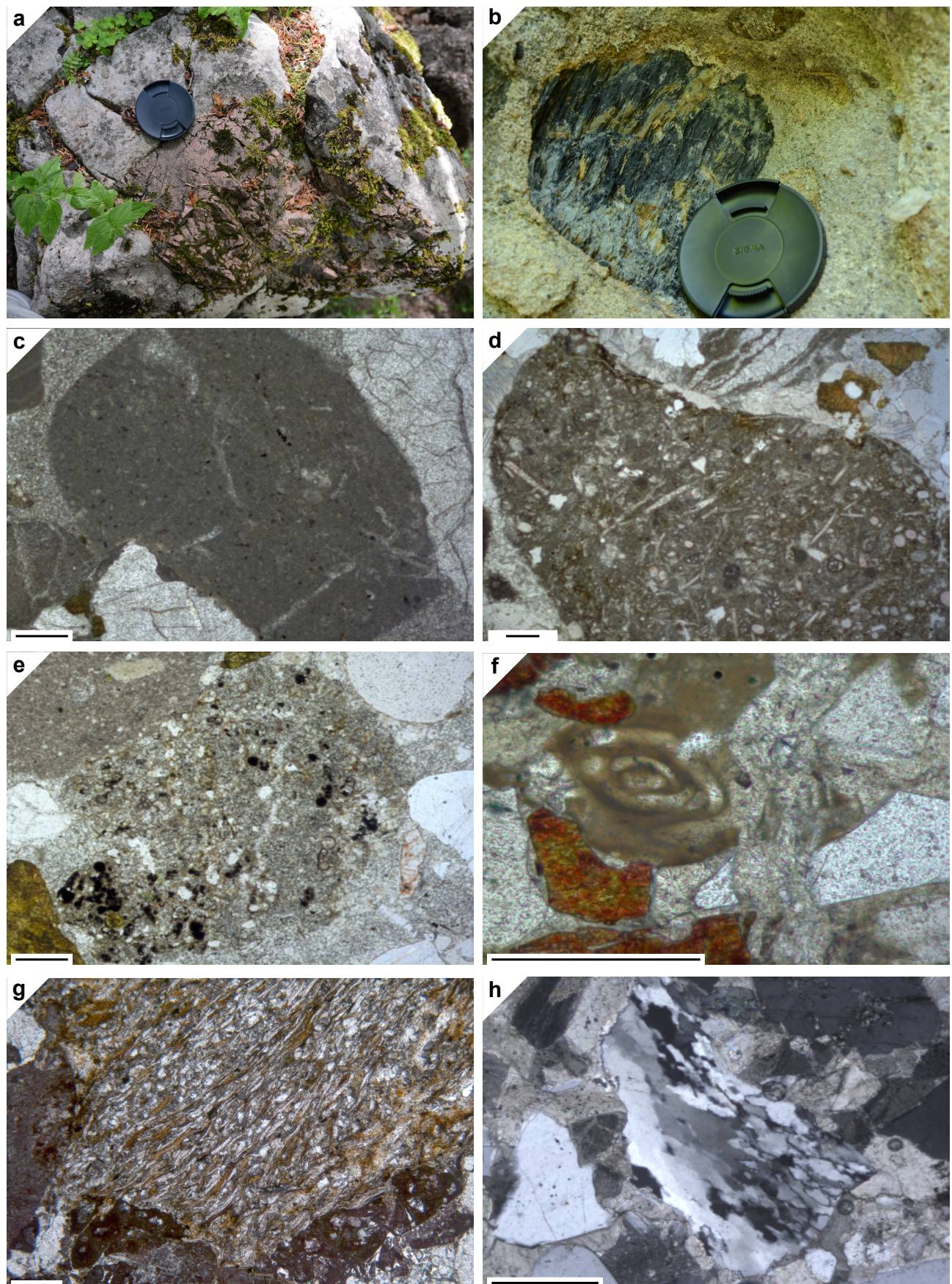


Figure 6: Microphotography and macrophotography of typical grains found in the Voiron Flysch: (a) pink granite fragment, (b) black Paleozoic sandstone fragment, (c) mudstone fragments, (d) foraminifera and bioclastic wackestone fragment, (e) siliciclastic wackestone, bioturbation filling ?, (f) phosphatized foraminifera, (g) metamorphic clasts with micaceous lineations, and (h) tectonized quartz polycrystalline grains. The black bar represents 200 μm .

Table 1: Additional key indices for the framework composition and heavy-minerals. Mineral abbreviations are based on the compilation of Whitney and Evans (2010) excepted: Qms = single monocrystalline quartz, Qps = non tectonised polycrystalline quartz, QpT = tectonised polycrystalline quartz, Ks = single K-feldspar, Ps = single plagioclase.

Key indices	Definition
Framework composition:	
$Qm = Qms + Qr$	Total monocrystalline quartz
$Qp = Qps + QpT$	Total polycrystalline quartz
$Qr = Qrg + Qrv + Qrm$	Quartz in rock-fragments
$Kr = Krg + Krv + Krm$	K-feldspar in rock-fragments
$K = Ks + Kr$	Total K-feldspars
$Pr = Prg + Prv + Prm$	Plagioclase in rock-fragments
$P = Ps + Pr$	Total plagioclases
$Lc = Lci + Lce$	Total calcareous lithic
$Lt = L + Qp$	Total lithics
$D = Ap + Grt + Hb + Rt + St + Zr$	Dense minerals
$M = Bt + Mu$	Total micas
$MI = Rm1/Rm \times 100 + Rm2/Rm \times 200 + Rm3/Rm \times 300 + Rm4/Rm \times 400 + Rm5/Rm \times 500$	Metamorphic index (Garzanti et al., 2004)
Zuffa classification:	
$NCE = Q + F + L + D + M$	Non Carbonate Extrabasinal grains
$NCI = Glt + FeO + P + Fph$	Non Carbonate Intrabasinal grains
$CE = Lce$	Extrabasinal calcareous grains
$CI = Lci + Bc$	Intrabasinal calcareous grains
Heavy-mineral:	
$LgM = Ep + Chl$	Low grade metamorphic heavy-minerals (Garzanti et al., 2004)
$HgM = St + And + Ky + Sil$	High grade metamorphic heavy-minerals (Garzanti et al., 2004)

The QEMSCAN® mineral phase identification relied on the combination of back-scattered electron (BSE) contrast and EDS spectra giving information on the elemental composition (Gottlieb et al., 2000). Individual X-ray spectra were compared to a library of known spectra and a mineral name was assigned to each individual acquisition point. The X-ray EDS spectra library, initially provided by the manufacturer, has been further developed in-house using a variety of natural standards. Measurements were performed on carbon-coated plugs that were adequately polished. Analytical conditions included a high vacuum and an acceleration voltage of 25 kV with probe current of 10 nA. The X-ray acquisition time was 10 ms per pixel using a point-spacing of 5 µm. Up to 122 individual fields of view were measured in each sample, with 1.5 mm per single field. QEMSCAN® data processing (e.g. unknown spectra debugging, particle boundary disambiguates, field stitching) was performed using the FEI iDiscover software. Composite mineral entries like garnet and tourmaline were defined by their respective EDS spectra consisted of individual elemental peak. Their intensities are defined by the ratios of measured elemental peaks and theoretical peaks representing a single pure compounds matter solely consisted of the element in question. Henceforth, the garnet entry comprises a comprehensive chemistry covering most of garnet species. Such a mean composition is defined by the following peak intensities: 35-200 (oxygen), 50-140 (aluminium), 80-210 (silicon), 20-210 (iron), 0-140 (magnesium), 0-100 (calcium) and Al/Si ratio that exceeded 0.3. Following the analogue reasoning the tourmaline composition used in this research consisted of oxygen (variable intensities), aluminium (140-280), silicon (120-220), sodium (0-45), magnesium (0-104), calcium (0-38), and iron (0-200), whereas fluorine and carbon may be encountered in EDS spectrum

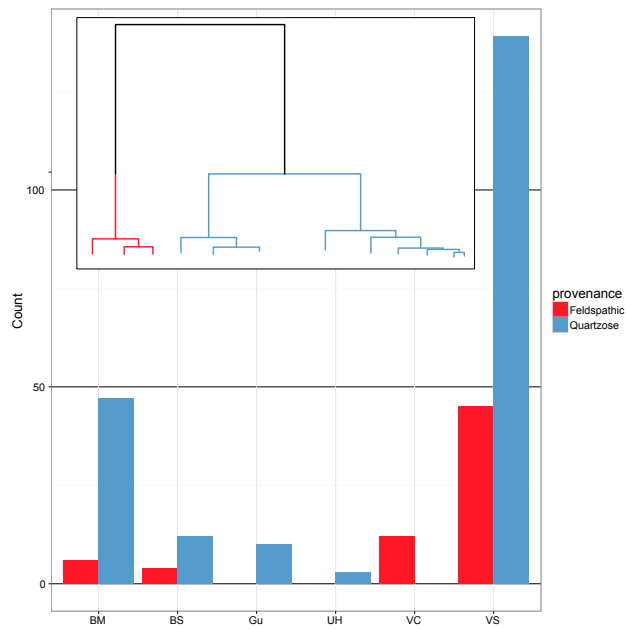


Figure 7: a) Relative proportion of the petrofacies within each stratigraphic unit. AS: Allinges Sandstone, BM: Boege Marl Fm., Gu: Other flyschs of the Gurnigel nappe, UH: Fenalet quarry (Ultrahelvetic ?), VC: Vouan Conglomerate Fm., VS: Voirons Sandstone Fm. b) Cluster tree diagram with the two identified petrofacies.

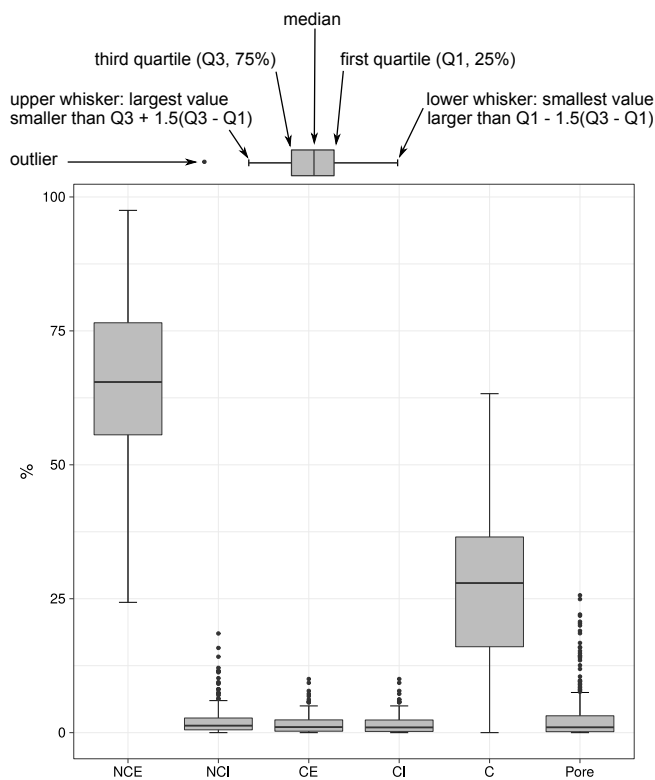


Figure 8: Box-whisker plot of the main grain classes of Zuffa (1980).

fitting the tourmaline entry compositional criteria. Garnet grains are organised into six different classes including melting phases: almandine, almandine-pyrope, almandine-pyrope-grossular, almandine-spessartine, grossular and undetermined garnets. Tourmaline grains are grouped into schorl, dravite and undetermined tourmaline. For each mineral group, the elemental composition of ten grains is extracted within each class and for each sample. In addition, 595 and 255 representative grains of garnet and tourmaline respectively were analysed by SEM-EDS system using an FEI QEMSCAN® Quanta 650F installed at the Department of Earth Sciences of the University of Geneva that was operated in the scanning electron microscope mode. The Bruker ESPRIT software was used for EDS spectra quantification in a standardless mode. Thereafter, garnet and tourmaline phase chemistry served as a basis to calculate the proportions of end-members of respective minerals using the spreadsheets designed by Andy Tindle from the Open University of Buckinghamshire for garnet (<http://www.open.ac.uk/earth-research/tindle/AGTWebPages/AGTSoft.html>).

The HMC (Heavy Mineral Content) and tHMC (transparent Heavy Mineral Content) indices of Garzanti and Andò (2007) provide the heavy mineral content in sandstone. They are based on the improved estimation of the H index of Baker (1962). A preliminary single garnet grain analysis was performed by QEMSCAN®. The different species of the garnet supergroup Grew et al. (2013) detected by QEMSCAN® are constrained to the most abundant species, the transitional solid-solution members and an undetermined group which gathers all the species not documented in QEMSCAN® database.

4.4 Thin section heavy mineral counting

Ten heavy mineral fractions (63–400 µm) from Ragusa (2009) were also recounted (Table ??). The protocol extraction is similar to those of the QEMSCAN® analysis, apart of the use of bromoform ($d = 2.89 \text{ g/cm}^3$) and the recovering by filtration. Thereupon, heavy mineral fractions were dried and placed on thin section. Total amount of 200 transparent heavy mineral grains was counted.

4.5 Data processing

Mineral abbreviations are based on the compilation of Whitney and Evans (2010) with a few exceptions like limonite (= Lim) to avoid confusion with metamorphic lithics (Lm). Additional grains are reported in Table ???. Computations and statistical analysis were performed using the R software (R Core Team, 2015). Samples distribution in a ternary diagram (Figs 9, 11, 17 and 19) is associated with fields indicating 90 % confidence regions for the distribution, calculated via Mahalanobis Distance and Log-Ratio transformation (Hamilton, 2016), which is more accurate and reliable (Weltje, 2002) than a hexagonal confidence area (Ingersoll, 1978). QEMSCAN® results were treated in FEI iDiscovery software v.5.2.

5 Results

5.1 Voirons Flysch framework composition

The dataset of the modal mineralogy of the Voirons Flysch is attached in supplementary data (Table A1). It describes raw data and stratigraphic affiliation for each sample. Samples are composed of poorly to well-cemented sandstones (Fig. 8). Sandstone beds mostly contain non-carbonate extrabasinal grains (NCE, 27.0 - 97.5 %), minor carbonate intrabasinal grains (CI, 0 - 11.13 %) and non-carbonate intrabasinal grains (NCI, 0 - 18.54 %). CI grains comprise a typical heterozoan assemblage including, in decreasing order, red-algae, foraminifers (e.g. nummulitids, discocyclinids, planktonic foraminifera), bryozoan and echinoid fragments, whereas the NCI grains consist of glauconite, phosphates (single grains and recrystallised foraminifers, Fig. 6e) and of some opaque minerals. Mudstone to wackestone lithoclasts were incorporated into the CI class, and consequently the proportion of carbonate extrabasinal (CE) grains is very low (≤ 2.5 %). Calcite cement mostly fills up interstitial voids (0 – 63.3 %) and porosity is usually very low, but may reach up to 25.6 % in few cases.

Cluster analysis on framework composition identifies two branches of different importance (Fig. 7). Based on their framework composition, the right branch (75.90 % of the samples) is determined as a Quartzose petrofacies, whereas the left branch (24.10 % of the samples) corresponds to a Feldspathic petrofacies. The Quartzose and Feldspathic petrofacies are mainly identified by distinctive Qm/F ratio (Figs. 9 and 10) with a slight overlap of the confidence areas. The incorporation of polycrystalline quartz (Qp) into the Q pole of the QFL diagram (Fig. 9a) emphasises their important proportion, flattening the scatter plot along the Q–F axis.

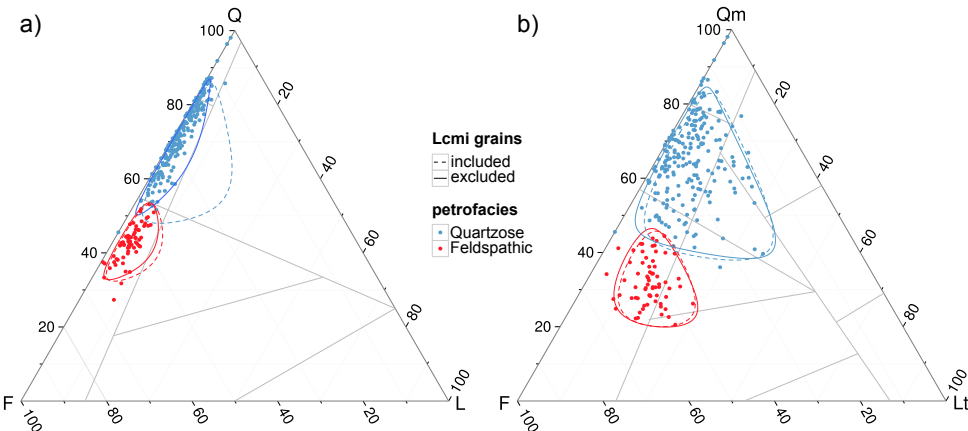


Figure 9: Petrofacies distribution in the QFL and QmFLt ternary diagrams of the Dickinson model.

5.1.1 The Quartzose petrofacies

The Quartzose petrofacies presents a high Q/F ratio (Fig. 10). The incorporation of mudstone to wackestone lithoclasts in the counting, especially in the QFL ternary diagram (Fig. 9a), reduces the strong influence of polycrystalline quartz in the samples of the Quartzose petrofacies. Considering the low lithic content and regarding the overall composition, the relative contribution of these micritic grains is low (Lc/QFL ratio, Fig. 10), which explains the similar distribution in the QmFLt ternary diagram (Fig. 9b).

The distribution of monocrystalline grains (Fig. 11a) shows a Qm–KP trend without a clear distinction within feldspars. The sample distribution is similar to that on QFL and QmFLt diagrams (Fig. 9), emphasising the strong influence of the Q/F ratio in the petrofacies. The distribution of quartz is shown in the ternary diagram QmsQpQr (Fig. 11b). Samples are concentrated around the Qm pole drawing a trend toward the Qr pole. The latter is mostly represented by a granitic source (Qrg/Qr ratio, Fig. 10). The Quartzose petrofacies is mature with a high proportion of monocrystalline quartz. The proportion of polycrystalline quartz is very low (Qp/Q ratio, Fig. 10), and the discrimination of the provenance is not as pronounced as in QFL (Fig. 9) and QpLsmLvm ternary diagrams (Fig. 11a). The composition of feldspar grains ranges from orthoclase to anorthite with a low albite content (Fig. 11c). However, a slight increase in the albite content, together with the alkali-feldspars, can be explained by the relative depletion of calcium plagioclase by albitisation, as already pointed out by Morad et al. (1990). Single grains represent the most abundant feldspar grains (Figs. 11d and 11e).

Several samples of the Quartzose petrofacies are devoid of lithic grains, and thus cannot be used in the analyses ($L = 0$, Fig. 10). The distribution of lithic fragments identifies a magmatic-sedimentary assemblage (Fig. 11d). However, the lithic grains are subordinate to the high content of polycrystalline quartz, as illustrated in the QpLsmLvm ternary diagram (Fig. 11e). The inclusion of mudstone to wackestone grains confers a more sedimentary-rich composition to the Quartzose petrofacies (Lc/L, Fig. 10). Sedimentary clasts are mostly represented by intrabasinal micritic limestone grains (Lcmi) presenting a large spectrum of textures from mudstones (Fig. 6c) to foraminifer- and bioclast-rich wackestones (Fig. 6d). The grain shapes are variable, from rounded to angular. Some micritic grains presenting a fuzzy boundary and containing quartz and glauconite (Fig. 6e) could possibly correspond to the filling of bioturbations. The lack of oxidised contours or other post-sedimentary weathering features (Zuffa, 1980) precludes an extrabasinal origin for these grains which are included in the CI grains as rip-up clasts reworked from the platform (Garzanti, 1991). Other sedimentary grains include chert debris, silt-size argillaceous fragments, and very rare recrystallised limestone clasts. The chemical and mechanical stability of chert fragments facilitates their persistence in the sedimentary record, which leads to overestimate their relative content. They could be an indicator of carbonate source rocks (Mack, 1984). Clayey to silty fragments are undoubtedly extrabasinal, but do not provide any information about their respective source. Sandstone fragments are usually absent as they directly provide single grains (e.g. quartz, feldspars). By contrast, conglomerate fragments were found in the conglomerate layers. Amber grains have been reported in the Allinges Sandstone (de Mortillet, 1863; Renier, 1893) and in the Vouan Conglomerate Fm. (Pilloud, 1936). Sparse phosphate grains and phosphatised foraminifers are also found (Fig. 6g), especially in the Boëge Marl Fm. No trend can be deduced from the sedimentary clasts as their distribution varies strongly

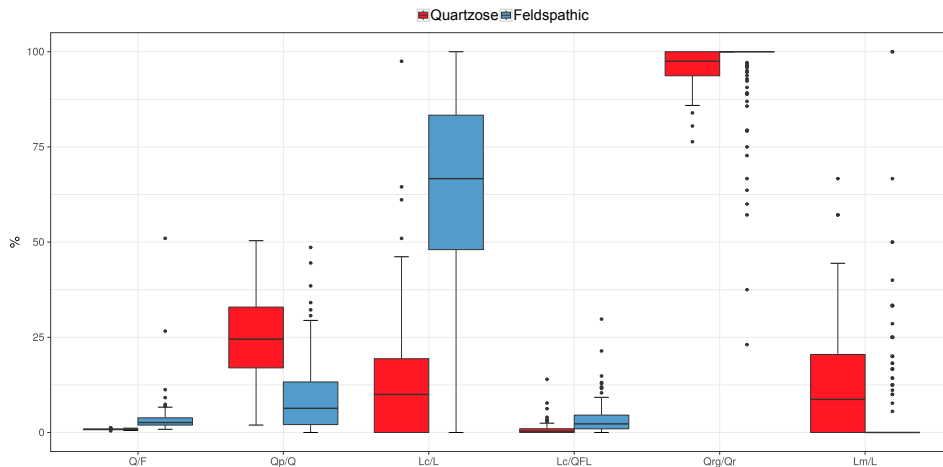


Figure 10: Box-whisker plot of the main ratio for the framework composition. For key to box plots see Fig. 8.

through the samples. The relative content of the CE grains in sandstone samples is very low (Fig. 8), which contrasts to their widespread occurrence in conglomerates (Cogulu, 1961; Winkler, 1983; Frébourg, 2006)). This may result either from (1) preferential dissolution, (2) late incorporation in the sedimentary process or (3) dilution by comparatively better-preserved igneous rocks.

Magmatic clasts are both of plutonic and volcanic origin. Most of the examined grains are plutonic rock-fragments (Fig. 11f), and plot in the granite to granodiorite fields, extending up to the tonalite field in some samples. Some microgranites were also encountered. The low proportion of volcanic grains precludes a reliable identification of volcanic-rock fragments. Samples plot in the quartz andesite to rhyolite fields (Fig. 11g), and andesitic lithoclasts have been reported in thin sections (Ospina-Ostios et al., 2013).

The Quartzose petrofacies is usually devoid of metamorphic grains (Lm/L ratio, Fig. 10). Thus, few points are plotted inside the ternary diagrams (Fig. 11h). They are concentrated near the end members or along the axis due to their scarcity. However, considering the mean values, the Quartzose petrofacies is preferentially located near the Rm5+ end member (High metamorphic grade). The Metamorphic index is low (Figs. 10 and 11i), and the Quartzose petrofacies presents also a low amount of tectonised polycrystalline quartz (Figs. 10 and 11j) which is typical of remnant oceanic deposits off-scraped at shallow levels (Garzanti et al., 2010).

5.1.2 The Feldspathic petrofacies

The Feldspathic petrofacies presents a low Q/F ratio (Fig. 10). Samples are not affected by the counting of mudstone to wackestone fragments (Fig. 8), which emphasises the scarcity of these grains in this provenance (Lc/L ratio, Fig. 10).

The Feldspathic petrofacies shows a high content in plagioclase among monocrystalline grains (Fig. 11a). Some albitionisation of plagioclase (Morad et al., 2000) is also observed as suggested by the minor content in albite (Fig. 11c). Quartz grains comprise an elevated content in lithic quartz grains (Fig. 11b, Qr) and polycrystalline quartz (Qp/Q ratio, Fig. 10). The latter usually originate from granitic rock fragments (Qrg/Qr ratio, Fig. 10), but gneisses cannot be excluded as an alternative source of polycrystalline quartz.

The Feldspathic petrofacies always contains a significant fraction of lithic fragments (Figs. 11d and 11e) including a large proportion of metamorphic lithoclasts (Lm/L ratio, Fig. 10), in addition to the magmatosedimentary assemblage. However, the lithic grains are less abundant than the polycrystalline quartz (Fig. 11e), and the confidence areas present a large overlap with the Quartzose petrofacies (Figs. 11d and 11e).

The magmatic lithic content is relatively similar to that described in the Quartzose petrofacies (Figs. 11f and 11g). Sample distribution overlaps the Quartzose petrofacies in the plutonic rocks (Fig. 11f). More volcanic rocks are observed in the Feldspathic petrofacies and plot in the Rhyodacite to Quartz-andesite fields (Fig. 11d). The Feldspathic petrofacies is characterised by significant inputs in metamorphic rock fragments (Lm/L ratio, Fig. 10) and a high MI index (Figs. 10 and 11i) dominated by high-grade, with subordinate low-grade, metamorphic lithics (Figs. 11i and 11j). However, such a high MI value is not common in remnant-ocean

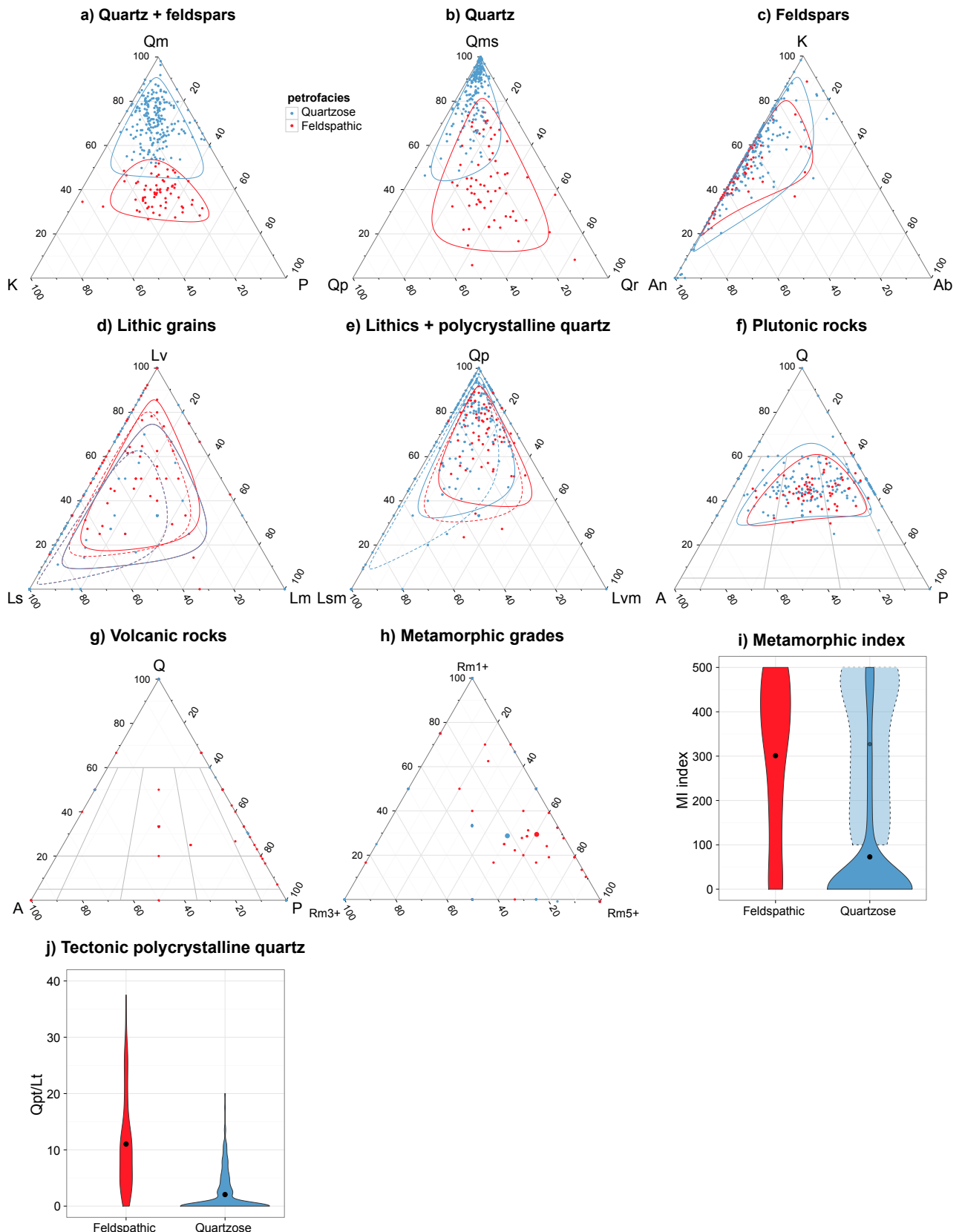


Figure 11: Monocrystalline grain distribution illustrated with overall composition (a) and dedicated distribution of quartz (b) and feldspars (c to e). Polycrystalline grain distribution illustrated with overall composition (f and g), estimated composition of plutonic (h), volcanic rocks (i) and metamorphic grades of Garzanti et al. (2004) (j). Metamorphic inputs are also evaluated with the MI index (Garzanti et al., 2004; Garzanti et al., 2010) (k) and the relative content of tectonic polycrystalline quartz (l).

deposits off-scraped at shallow depth (Garzanti et al., 2010; Fig. 8). Protoliths likely consist of sedimentary rocks according to the nomenclature of (Garzanti and Vezzoli, 2003). Tectonised polycrystalline quartz (QpT) stands for a reliable indicator of the supply of metamorphic rock fragments (Young, 1976; Figs. 10 and 11j). The metamorphic clasts, especially schists, are more easily crushed during the sediment transport Picard and McBride (2007).

5.2 Voirons Flysch heavy-mineral assemblage

The dataset of the heavy minerals of the Voirons Flysch is summarised in Table ?? and Table ?? for the QEMSCAN® analyses and the samples from Ragusa (2009) respectively. The abundance of heavy minerals and transparent heavy minerals (HMC and tHMC) in the 63–125 µm fraction is poor to moderately poor (sensu Garzanti et al., 2010) in both petrofacies (Fig. 12; Table ??). The small gap between HMC and tHMC indices illustrates an elevated content of transparent heavy minerals (tHM). The assemblage of tHM represents 60 to 90 % of the dense minerals followed by opaque grains and micas (Ragusa, 2015). The lowest content in tHM is found in the distal density-current deposits (JR5 and JR57), and is associated with a higher mica content (Fig. 13). In both grain-size range, transparent heavy minerals are represented by ultrastable (ZTR group) and stable (garnet and apatite) species in both petrofacies (Fig. 14). Accessory grains of the tHM trace group consist of unstable minerals (e.g. barite, epidote, pyroxene and hornblende).

There is some discrepancies between the both fractions. The main difference lies in the relative distribution of the mineral species (e.g. higher zircon and lower rutile content in the 63–400 µm). Rutile and titanite are relatively more abundant in the 63–125 µm fraction than staurolite, tourmaline and zircon and inversely in the 63–400 µm fraction. These differences may derive from inherited grain-size in source rocks (Morton and Hallsworth, 1999). In addition, the QEMSCAN® determination may also influence the relative proportion with a better identification of the finest fraction which is more difficult to constrain with an optical microscope. Despite these discrepancies, the relative abundance of some diagnostic species (e.g. garnet), or dedicated ratios discriminate Quartzose and Feldspathic petrofacies in both grain-size ranges (Figs. 12 and 14).

5.2.1 The Quartzose petrofacies

The Quartzose petrofacies essentially contains abundant tourmaline reflected by lower ATi (Morton and Hallsworth, 1994) and higher ZTR indices (Fig. 12; Table ??). The garnet content is low, as emphasised by the low GZi index (Fig. 12; Table ??; Morton and Hallsworth, 1994). The scarce K-rich volcanic glass confirms the rhyolitic source described in Fig. 11g. A large variation in mica distribution and the occurrence of biotite characterise the Quartzose petrofacies.

Preliminary single-grain analysis on garnets identified almandine and almandine-pyrope solid solution (mean = 86.09 %) as dominant phases (Fig. 15a). Subordinate grains are almandine-pyrope-grossular and almandine-spessartine solid solutions (mean = 6.95 %). Less than 10 % of garnets grains were undetermined. Moreover, the Quartzose petrofacies shows the schorl-dominated assemblage among tourmaline grains (Fig. 16).

5.2.2 The Feldspathic petrofacies

The Feldspathic petrofacies is characterised by a high content in garnet and an elevated GZi index in the 63–125 µm fraction (Fig. 12, Table ??). Consequently, the ATi index is high and the ZTR index is low (Fig. 12; Table ??). The distribution of micas is relatively constant in the Feldspathic petrofacies and is dominated by chlorite (Fig. 13). Single grain analysis on garnet identified almandine-pyrope-grossular and almandine-spessartine solid solutions, similar to the assemblages found in the Quartzose petrofacies. As for the latter, the tourmaline assemblage is dominated by schorl (Fig. 16).

5.2.3 Garnet and tourmaline geochemistry

The geochemical data of garnet and tourmaline are summarised in supplementary data (Tables A3 and A4 respectively). Both petrofacies share similar garnet distribution dominated by almandine (Alm) and almandine-pyrope (Alm-Prp) varieties (Fig. 15a). The relative composition of each class is summarised in Fig. 15c. Several classes contains a minor amount of andradite. The almandine-spessartine phase (Alm-Sps) includes a minor content in grossular. Undetermined garnets correspond to spessartine-almandine-grossular (Sps-Alm-Grs).

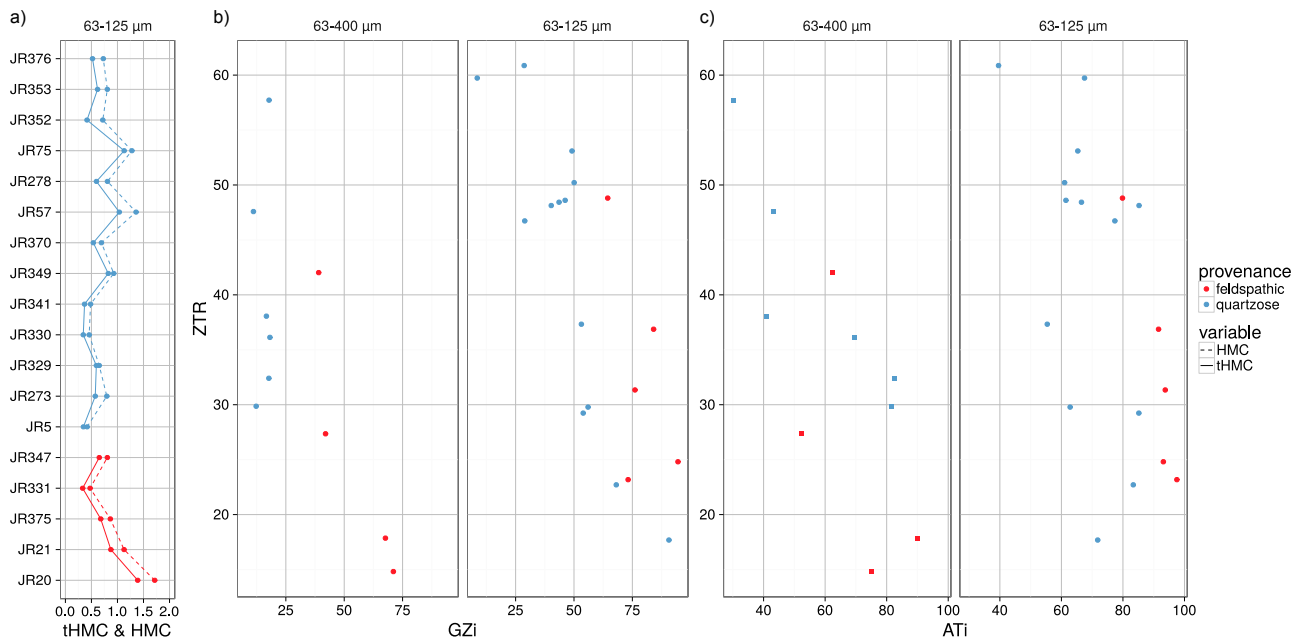


Figure 12: Heavy mineral indices. (a) tHMC: transparent heavy mineral content (Garzanti and Andò, 2007), (b) ZTR versus GZi (garnet/garnet+zircon) and (c) ZTR versus ATI (apatite/apatite+tourmaline) from Morton and Hallsworth (1994)

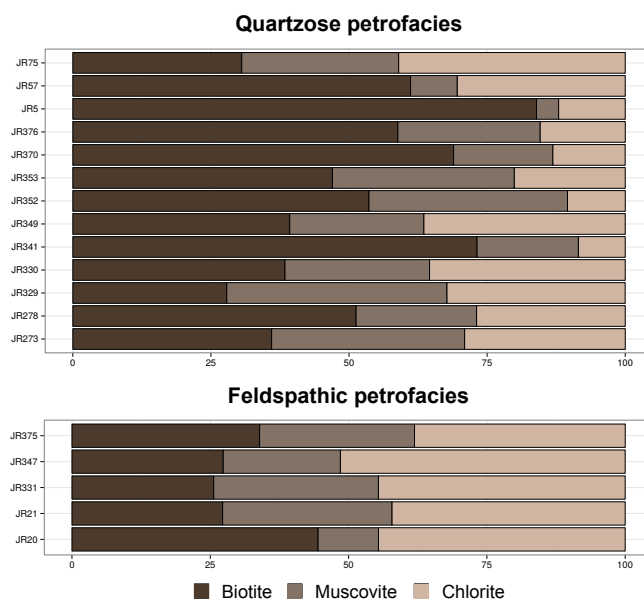


Figure 13: Mica distribution in the 63–125 µm fraction

Finally grossular (Grs) is relatively pure (> 80 %) with few amount of andradite. Almandine-pyrope-grossular (Alp-Prp-Grs) is also reported in trace amount. Both petrofacies contain also a similar tourmaline composition dominated by schorl (Srl) and secondary dravite (Drv) (Fig 16). Undetermined tourmaline identified by the QEMSCAN® correspond to Drv-rich Srl. Tourmaline geochemistry shows a wide compositional variation governed by Fe content.

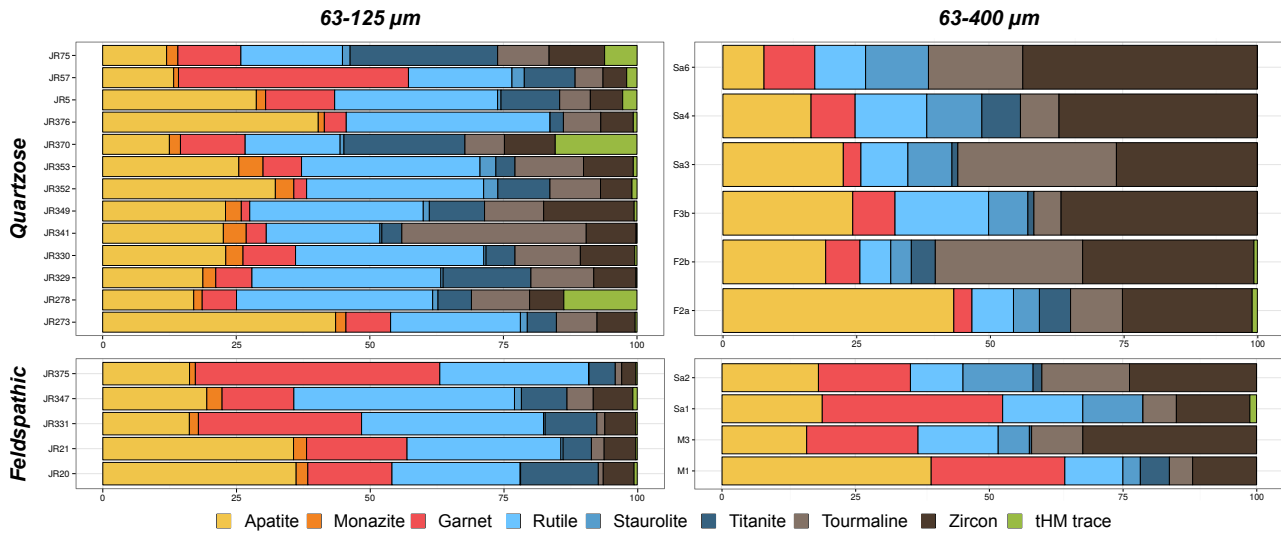


Figure 14: Transparent heavy-mineral distribution for the 63–125 µm and recounted 63–400 µm fractions

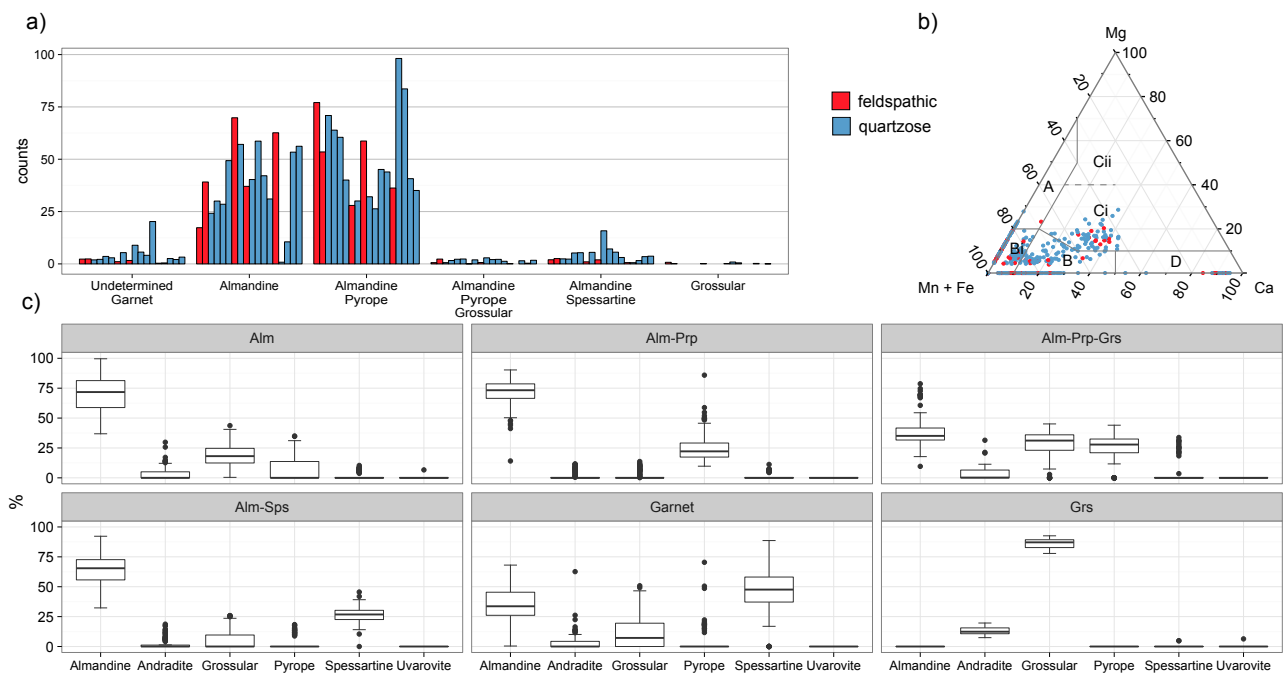


Figure 15: Garnet geochemistry. a Relative distribution of the different classes identified by the QEMSCAN®, b ternary diagram of garnet discrimination after Mange and Morton (2007), c SEM-EDS composition of the different garnet classes based on end-member abundances. For key to box plots see Fig. 8

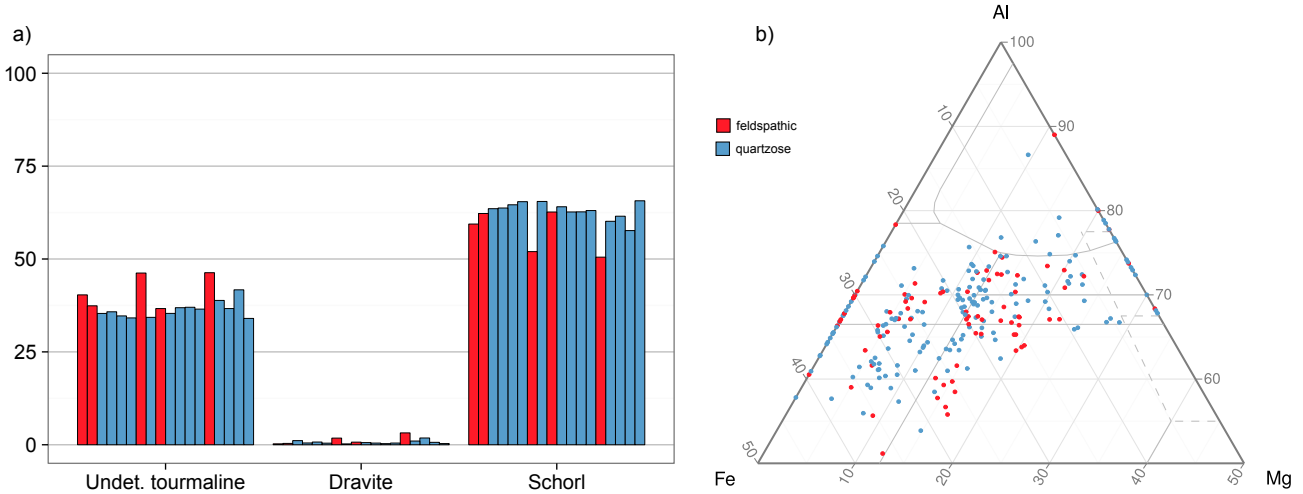


Figure 16: Tourmaline geochemistry, a relative distribution of the different classes identified by the QEMSCAN®, b ternary diagram of tourmaline discrimination after Henry and Guidotti (1985)

6 Discussion

6.1 Petrofacies distribution in the stratigraphic subdivisions of the Voiron Flysch

As mentioned previously, the stratigraphic units of the Voiron Flysch were up to now poorly differentiated from a petrographic viewpoint (Lombard, 1940; Van Stijvenberg, 1980; Charollais et al., 1998). Our modal composition analysis demonstrates that the Vouan Conglomerate Fm. is restricted to the left branch of the cluster tree (Fig. 7), and shows a homogeneous composition (Fig. 9). It thus represents the most typical stratigraphic unit of the Feldspathic petrofacies. However, several samples from other formations, especially from the Voiron Sandstone Fm., are located on the same branch as the Vouan Conglomerate Fm. (Fig. 7). The feldspatho-quartzose lithic composition of these samples strongly differs from the other samples of these formations, and rather corresponds to the Vouan Conglomerate Fm. They consist of single beds, randomly distributed in the Voiron Sandstone Fm., in the Boëge Marl Fm. and in the Bruant Sandstone Fm. (Fig. 17). They are numerous near the boundary between the Voiron Sandstone Fm. and the Vouan Conglomerate Fm. which suggests an interlayering rather than a tectonic contact between these two units (Fig. 17). The other lithostratigraphic units of the Voiron Flysch are characterised by the Quartzose petrofacies (Fig. 7). The latter represents the major source of detritus of the Voiron Flysch, and presents a wide spectrum of composition controlled by the depositional settings in a deep-sea fan (Ragusa, 2015). The Quartzose petrofacies of the crest conglomerates (e.g. “Conglomérat de Pralaire”; Lombard, 1940; Fig. 4) precludes an affiliation with the Vouan Conglomerate Fm., as stated by (Van Stijvenberg, 1980).

It is impossible to recognise the provenances from the observation of sandstone beds in the field, unless they are interstratified with conglomerate layers comprising typical lithoclasts (e.g. pink granite fragments for the Quartzose petrofacies and black sandstone clasts of Paleozoic age for the Feldspathic petrofacies). Hence, the localisation of the Feldspathic petrofacies in single beds of the Voiron Flysch and the fine-tuning of the boundaries of the Vouan Conglomerate Fm. remains problematic. In addition, these new data modify the stratigraphic affiliations of some outcrops (Ragusa, 2015). In particular, the framework composition of the deposits exposed in the Fenalet quarry indicates that they must be correlated with the Voiron Flysch, and not with the Ultrahelvetic units.

6.2 Provenance of the Quartzose petrofacies

The quartz-rich composition and low HMC values of the Quartzose petrofacies correspond to the Transitional continental to Mixed tectonic settings (Fig. 9) of the Dickinson model (Dickinson, 1985; Dickinson and Suczek, 1979). Rock composition describes a low unroofed basement source including crystalline rocks and a sedimentary cover. The occurrences of zircon, tourmaline, xenotime, and monazite are common in intermediate to acidic granite and their metamorphic counterparts as well as in polycyclic detrital sandstones (Fig. 14; Mange and Maurer, 1992; Stefani et al., 2007; von Eynatten and Dunkl, 2012). Tonalite composition is confirmed by the

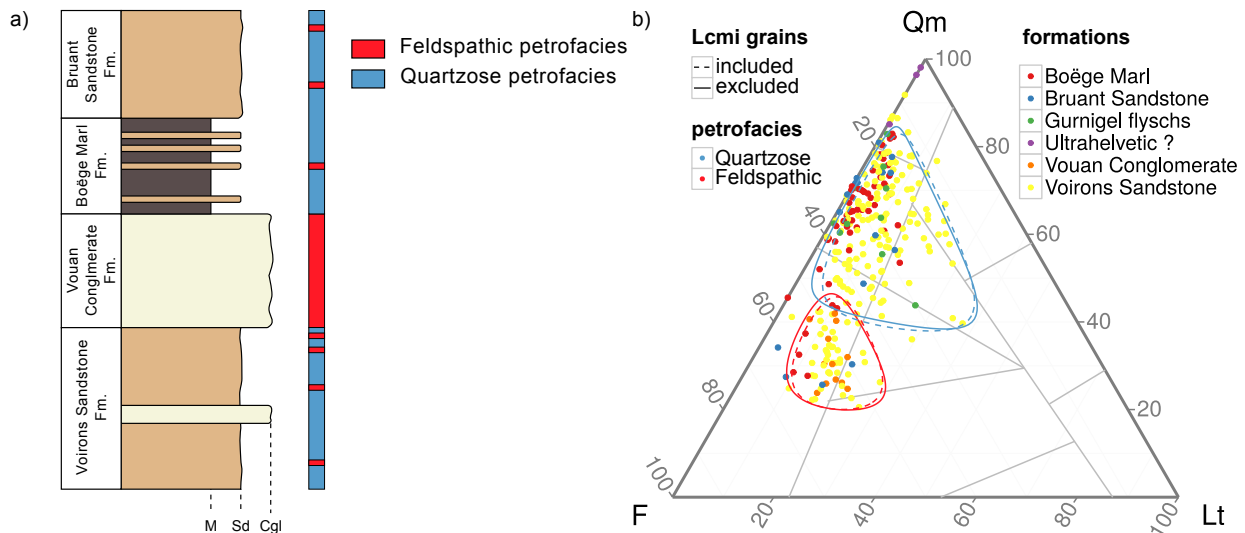


Figure 17: Relationship between petrofacies and stratigraphic units illustrated by a synthetic log of the Voirons Flysch (a) and the QmFLt ternary diagram (Fig. 8b) with the initial stratigraphic affiliation (b). Note the widespread location of most of the stratigraphic units

high ATI index (Fig. 12; Büttler et al., 2011) and the negative correlation of apatite with silicates (von Eynatten and Dunkl, 2012). Occurrence of andesite grains has also been reported (Ospina-Ostios et al., 2013). Tourmaline grains plots in fields 2, 3, 4 and 5 of the ternary discrimination diagram (Henry and Guidotti, 1985; Fig. 16b), suggesting a wide range of source rocks. The latter include igneous rocks (fields 2 and 3) and metasedimentary rocks (fields 4 to 6) Henry and Guidotti (1985); Mange and Maurer (1992). In addition, the minor amount of dravite further suggests igneous rocks as the main source of tourmaline (Fig. 16a). Sedimentary inputs have probably been underestimated, and might contribute a lot to the detrital sedimentation (Picard and McBride, 2007). The ZTR index suggests an important reworking of detrital sedimentary rocks (Fig. 12). Sedimentary clasts found in conglomerate layers originate from a carbonate-rich stratigraphic succession of Triassic to Cretaceous age (Ragusa, 2015). Further analyses are needed to better constrain the source of some peculiar facies (e.g. neritic carbonates similar to Urgonian Limestones; Lombard, 1940). Likewise, the widespread occurrence of phosphate in the Tethyan realm from the Cretaceous to the Eocene (Broudoux, 1985; Notholt et al., 1989; Follmi, 1990) is not a reliable indicator of a palaeogeographic origin. Amber grains are also found in other locations of the Gurnigel nappe (Tercier, 1928), and correspond to a fluvial or coastal source. They do not relate to a particular palaeogeographic origin.

Our petrographic data (quartz-rich assemblage, high ZTR index) further suggest that the Quartzose petrofacies is very mature, and experienced polycyclic sedimentation, as confirmed by its location in the Mixed field of the Dickinson model (Fig. 9). This may occur in a fluvial system by the migration of the river bed (Amorosi and Zuffa, 2011) or in marine basins through the influence of an oceanic current (Morton and Hallsworth, 1999). Likewise, the scattered presence of metamorphic fragments (Figs. 11h and 11i) could also result from the reworking of deposits related to the Feldspathic petrofacies. Following the Garzanti model (Garzanti et al., 2007), the Quartzose petrofacies provenance can correspond either to the Continental block or to the Clastic wedge provenance.

Intrabasinal components, including chemical (glauconite and phosphate) and biological (bioclasts and micritic limestones) grains, are frequent in the samples from the Quartzose petrofacies. They indicate the reworking of platform sediments by gravity currents, especially during transgressive phases (Odin and Matter, 1981; Garzanti, 1991). A high amount of carbonate grains is characteristic of close-up basins (Critelli et al., 2007), and controls diagenetic processes such as cementation and porosity reduction (Fig. 18). The reworking of sediments could also be explained by the influence of marine currents (Ingersoll, 1990; Ingersoll et al., 1993) especially during sea-level highstands (Amorosi and Zuffa, 2011). Hence, both allochthonous and autochthonous factors controlled the composition of the Quartzose petrofacies.

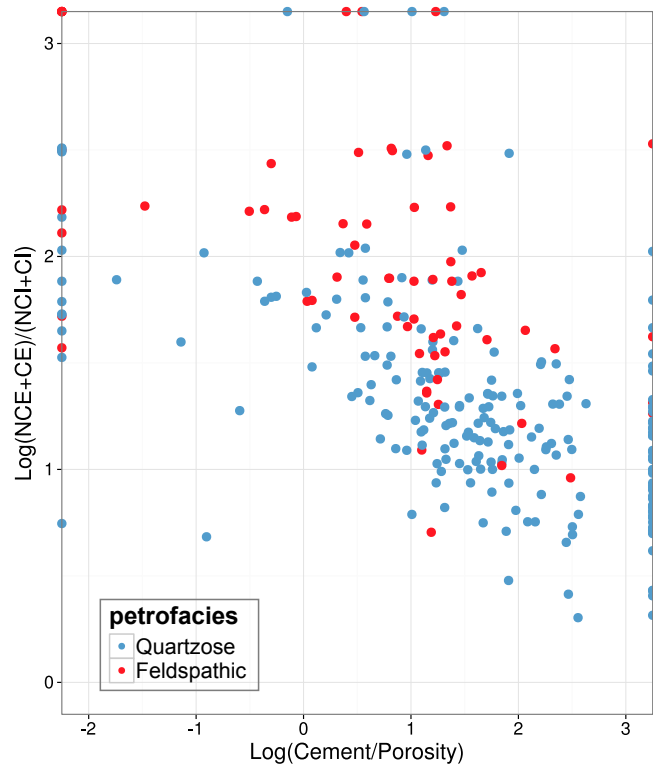


Figure 18: Relationship between extrabasinal vs. intrabasinal grains and cement vs. porosity

6.3 Provenance of the Feldspathic petrofacies

The feldspar-dominated (Fig. 9) assemblage indicates a location in the Basement uplift to Dissected volcanic arc fields of the Dickinson model (Dickinson, 1985; Dickinson and Suczek, 1979). However, the source rocks are quite similar to those of the Quartzose petrofacies (Figs. 11 and 14). The main difference lies in the low sediment maturity in the Feldspathic petrofacies. Hence, it presents a lithic-rich composition (Figs. 9 and 11) with some andesitic and granitic rock fragments. The main characteristic of the Feldspathic petrofacies is the abundance of metamorphic lithics and rock fragments in sand-size grains (Fig. 11), and especially of the psammite-derived metamorphic lithics according to the colour guide of (Garzanti and Vezzoli, 2003). Polycrystalline quartz (QpT) is a good indicator of these metamorphic inputs (Fig. 11d). The occurrence of staurolite (amphibolite facies), rutile (HP grade) (Fig. 14) and chlorite (low grade metamorphism) (Fig. 15) suggest a large variability of metamorphic rocks. They are presumably related to regional metamorphism and to low- to intermediate-grade meta-sediments (von Eynatten and Gaupp, 1999; Copjaková et al., 2005; von Eynatten and Dunkl, 2012). The association of garnet and staurolite may indicate a source in micaschist complexes (Füchtbauer, 1964). According to the (Mange and Morton, 2007) garnet discrimination diagram (field Bi, Fig. 15b), the almandine-dominated garnet distribution (Alm and Alm-Prp) mostly corresponds to amphibolite-grade (MP-MT) metasedimentary rocks, thus corroborating the high metamorphic grade (Figs. 9e and 9f). The small amount of Alm-Sps and Sps-Alm-Grs could derive from granites and pegmatites or from metamorphic rocks such as higher greenschist facies (Krippner et al., 2014, field B Fig. 15b), whereas the scarce Grs may originate from contact metamorphosed marls or calcareous shale (Win et al., 2007). Besides, the low amount of pyrope precludes peridotite and eclogite source rocks (von Eynatten and Gaupp, 1999).

The high amount of metamorphic grains correlates the Feldspathic petrofacies with the Axial belt provenance (Garzanti et al., 2004, 2007, 2010). Such a provenance favours the entrainment of fresh material in the sedimentary cycle. However, the similarity with the Quartzose petrofacies strongly suggests that sediments of both petrofacies met comparable weathering conditions, regarding the scarcity of the other typical metamorphic unstable grains.

Intrabasinal grains (NCI and CI grains) are scarce in the Feldspathic petrofacies (Fig. 18) suggesting a reduced marine influence in the sand composition and a sparse cementation linked to the low carbonate content. Hence, alloigenic factors, especially tectonics, controlled sediment composition of the Feldspathic petrofacies. This may explain the formation of this relatively unaltered proximal facies which is usually

associated to sea-level lowstands (Amorosi and Zuffa, 2011).

6.4 Regional comparison with the other Prealps flyschs

Our data are compared with the following flysch deposits exposed in the Prealps (Figs. 1, 2 and 3): (1) the Upper Prealps flyschs (Caron, 1972; Flück, 1973; Gasinski et al., 1997) represented by the Sarine, the Dranses and the Simme flyschs – South Penninic domain, (2) the Médianes Flysch (Flück, 1973; Caron et al., 1989) – Briançonnais domain, (3) the other flyschs from the Gurnigel nappe represented by the Schlieren (Winkler, 1983, 1984) and the Wägital flyschs (Winkler et al., 1985a) and (4) the Niesen flyschs (Ackermann, 1984, 1986) – Valais domain. The petrography of these units has been studied during the 1970–1980's following the Gazzi-Dickinson method (Fig. 19), and salient results are compiled in Caron et al. (1989).

The first phase of flysch deposition in the Alps is represented by the Simme and the Gets flyschs. They are devoid of garnet grains, but contain a variable amount of chrome-spinel (Fig. 20a) which is inherited from the Piemont ophiolites (Bertrand and Delaloye, 1976; Bill et al., 1997; Beltrán-Triviño et al., 2013). Their lithic-rich composition (Fig. 19a) emphasises massive inputs of fresh material from both continental and oceanic crusts (Gasinski et al., 1997, and references therein). Framework composition describes a Recycled orogen tectonic setting (Dickinson and Suczek, 1979) and an Ophiolite provenance (Garzanti et al., 2007), considering the spinel-rich heavy minerals. They do not share any petrographic similarities with the flyschs from the Gurnigel nappe (Fig. 19a).

The younger Sarine and Dranses flyschs have a similar framework composition characterised by a low lithic content (Fig. 19a). However, the heavy mineral populations are very different from the Simme and the Gets flyschs (Fig. 20a). The low garnet content indicates minor metamorphic inputs, whereas the high proportion of zircon and tourmaline indicates a granitic source. These flyschs plot in the Continental Block to Clastic wedge provenance according to the Garzanti model (Garzanti et al., 2007). Their location in the Transitional continental to Mixed tectonic settings (Dickinson and Suczek, 1979; Dickinson, 1985), as well as the low garnet content, is similar to that of the Quartzose petrofacies (Fig. 19a).

The composition of the Médianes Flysch is characterised by a feldspar-dominated composition. Garnet grains occur in the heavy-mineral assemblage of this flysch, but seems to be missing in the Brèche Flysch (Fig. 15). The rare chrome-spinel grains found in the Médianes Flysch (Flück, 1973) are likely reworked from the Simme or the Gets flyschs (Beltrán-Triviño et al., 2013). Provenance interpretation defines a Basement uplift tectonic setting (Dickinson and Suczek, 1979; Dickinson, 1985). The composition of the Médianes Flysch is very similar to the Feldspathic petrofacies of the Voirons Flysch, but is richer in lithic fragments (Fig. 14b). Scarce data from the Brèche Flysch precludes any provenance interpretation.

The Schlieren and Wägital flyschs plot in the Transitional continental to Mixed fields of the Dickinson model. These units appear to differ from the Quartzose petrofacies because of the different interpretation of micritic lithoclasts and by a richer content in polycrystalline quartz. Incorporation of the micritic grains (Fig. 15c; dashed lines) in the counting provides similar results. The Wägital Flysch is characterised by an elevated content in metamorphic and volcanic lithoclasts. Garnet and staurolite contents are high, and equivalent to the zircon + tourmaline content. The Schlieren Flysch is rich in sedimentary lithoclasts, with the notable presence of dolostone fragments likely derived from Triassic deposits (Winkler, 1983, 1984). Metamorphic inputs decrease, and the granitic source rather influences the heavy-mineral assemblage. Based on the ATI values (Büttler et al., 2011), two different magmatic provenances are reported for the Schlieren Flysch: a granitic-rhyolitic source and a tonalitic-andesitic source. The Niremont Flysch shows a particularly elevated content in apatite and garnet associated with a low content in ultrastable minerals (Fig. 20). No framework composition is available for this flysch.

The overall composition of the flyschs from the Gurnigel nappe share many similarities, and confirm the uniqueness of this nappe (Fig. 19c). The heavy-mineral population consists of a garnet + ZTR-dominated assemblage and a variable amount of apatite in all these flysch deposits (Fig. 20; Wildi, 1985). However, differences in the lithoclast distribution (Fig. 14c) suggest a compositional variation from East to West (Winkler, 1984), which may indicate a lesser unroofed basement source in the West. However, this does not appear in the heavy-mineral distribution. Hence, the composition evolves from a magmatic and metamorphic source in the East to a more sedimentary-rich supply in the Voirons Flysch (Fig. 19c, QpLvmLsm diagram), showing that the crystalline sources are progressively diluted by a greater amount of sedimentary detritus.

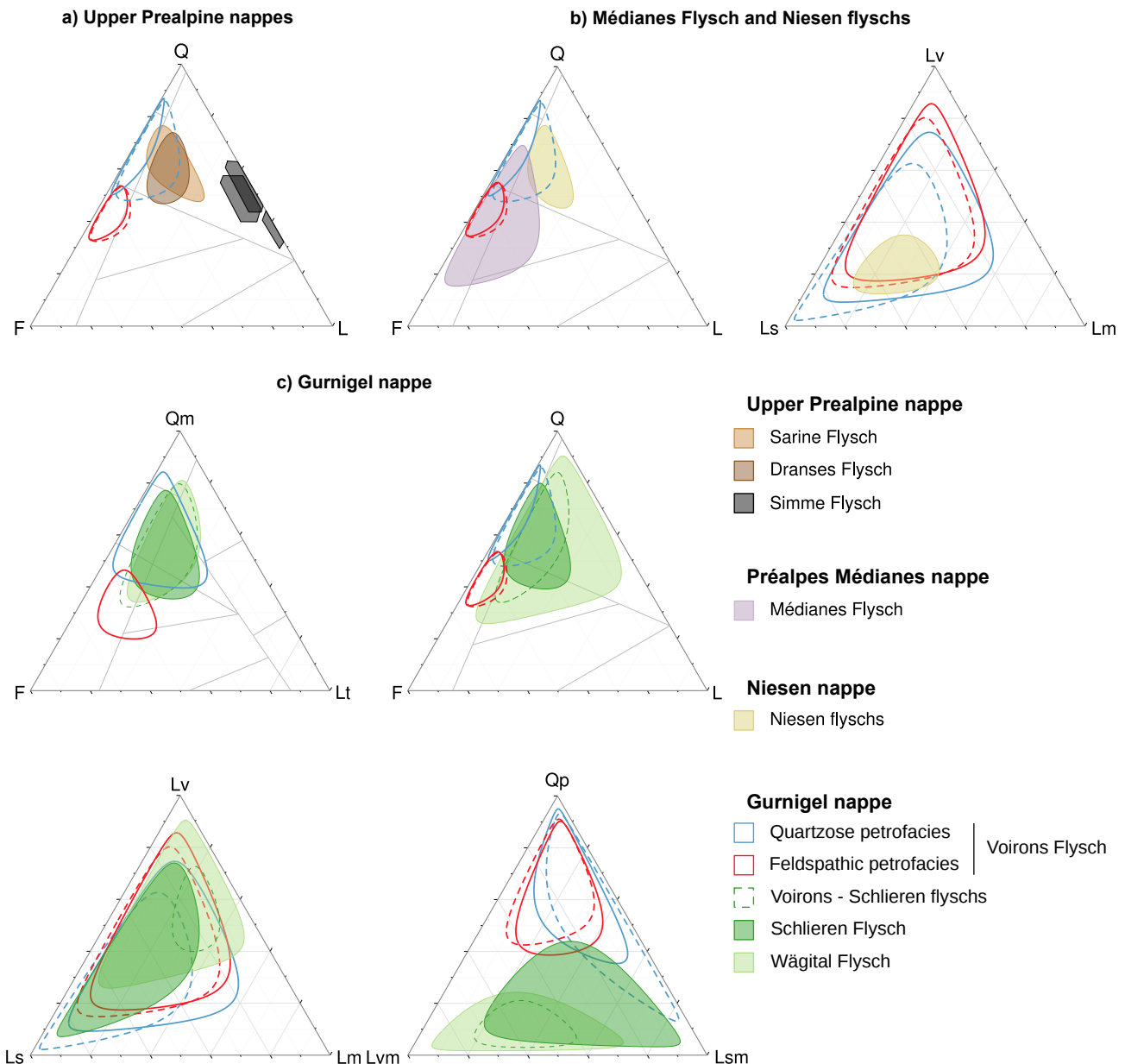


Figure 19: Ternary diagrams of the Dickison model of the Voirons Flysch provenances compared to the Upper Prealps flyschs (a), the Médianes Flysch and the Niesen flyschs (b) and the other Gurnigel flyschs (c). See references in text

The similar framework composition and heavy-mineral assemblage confirm the affinity of the Quartzose petrofacies from the Voirons with the rest of the Gurnigel nappe (Fig. 19c). The occurrence of samples from the Fayaux and Zollhaus quarries in this branch confirms the similarity of this source with the detrital sources reported for the other flyschs of the Gurnigel (Winkler, 1983, 1984; Caron et al., 1989), which is also corroborated by the presence of pink granite fragments (Fig. 6a). However, based on the ATI values (Fig. 12), the granitic-rhyolitic source of the Schlieren Flysch (Bütler et al., 2011) is not present in the Voirons Flysch. The large distribution of the Wägital Flysch slightly overlaps the Feldspathic petrofacies, and the content in metamorphic lithics shows some affinity which cannot be further resolved. However, the massive Vouan Conglomerate Fm. is not reported from any other flysch deposits in the Gurnigel nappe (Caron et al., 1989). The lack of pink granite pebbles in this formation further demonstrates the quasi-uniqueness of the Feldspathic petrofacies in the Voirons Flysch.

The zircon geochronology (Beltrán-Triviño et al., 2013) and the lack of garnet (Wildi, 1985; Bernoulli and

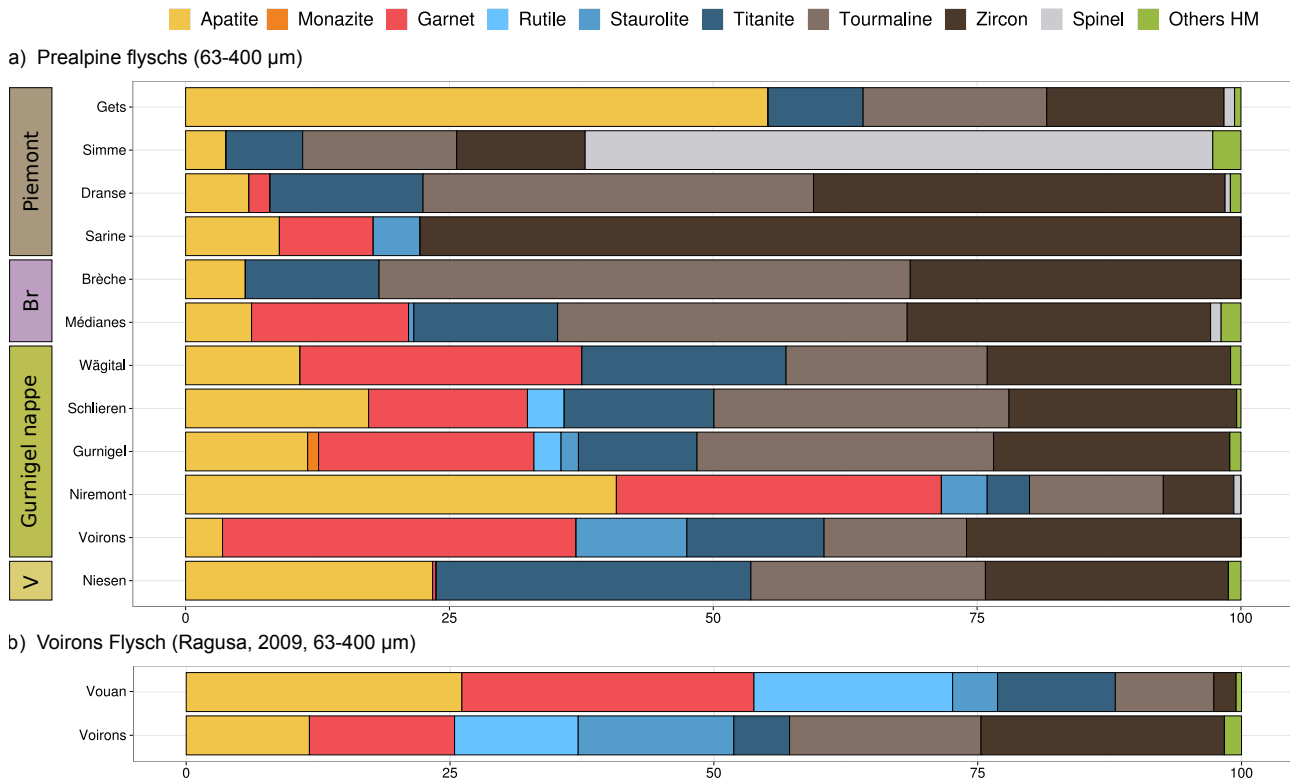


Figure 20: Transparent heavy-mineral distribution in the Prealps flyschs (a) and mean distribution from the Voirons Flysch (Ragusa, 2009, 63–125 µm and 63–400 µm range (Ragusa, 2009, modified) (b). Br Briançonnais domain, V Valais domain. See references in text

Winkler, 1990; Argnani et al., 2004) indicate a detrital source located along the northern Tethyan margin for the Niesen flyschs (Wildi, 1985). Despite the distinctive detrital provenances, no significant differences in the QFL ternary diagram have been observed between these flyschs and those from the Gurnigel nappe (Fig. 19b). These similarities are linked to the homogeneous composition of rock sources along the northern margin of the Alpine Tethys characterised by granitic rocks and sedimentary covers shared with the Ultrahelvetic realm (Ackermann, 1986; Lihou and Mange-Rajetzky, 1996).

This review emphasises the similar framework composition and heavy-mineral assemblage of several Prealps flyschs derived from the southern Tethyan margin: the Dranses Flysch, the Sarine Flysch, the Médianes Flysch and the flyschs from the Gurnigel nappe. Such resemblances result not only from similar rock sources, but also from the cannibalisation of these flyschs that were progressively incorporated into the sedimentary accretionary prism, and fed the subsequent flysch deposits. They also suggest a gradual tectonic evolution of the accretionary wedge and the surrounding crystalline basement (Fig. 21). Sedimentary inputs were initially dominated by stable-rich grains (e.g. ZTR province of Wildi, 1985) originating from plutonic crystalline basement and sedimentary covers. Punctual reworking of oceanic crust (e.g. Cr-Spinel province of Wildi, 1985) indicates that residual ophiolite were exposed in front of the southern Tethyan margin (Gasinski et al., 1997). They were progressively replaced and/or associated with metamorphic rock source related to the uplift of the metamorphic belt (e.g. Garnet province of Wildi, 1985). The transition ZTR to Garnet province should be related to the closure of the Piemont Ocean and the subduction of the Briançonnais microcontinent.

Considering the framework composition and heavy-mineral assemblage, the Quartzose petrofacies could have been fed by the Dranses and/or the Sarine flyschs, whereas the Feldspathic petrofacies could originate from the Médianes Flysch. Finally the different composition within the Gurnigel nappe emphasises different sedimentary systems inherited from the tectonic deformation of the sedimentary accretionary prism.

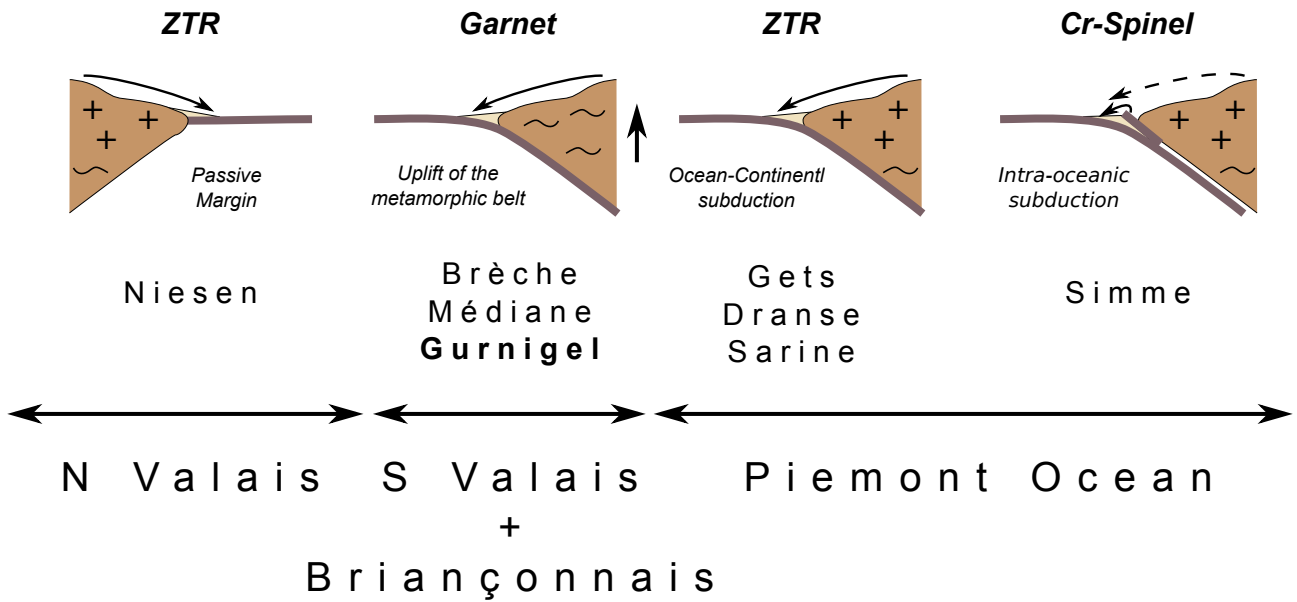


Figure 21: Synthetic model of the evolution of tectonic settings during the Tethyan close-up and the respective heavy-mineral provinces of (Wildi, 1985)

6.5 Geotectonic model of the Voirons Flysch

The petrographic and mineralogical data presented in this study show that, like the other flyschs of the Gurnigel nappe, the constituent material of the Voirons Flysch originates from the southern margin of the Alpine Tethys (Bütler et al., 2011). Five major age populations were identified in the detrital zircons (610-550, 510-490, 468-425, 346-315, 205 Ma; Fig. 23; Bütler et al., 2011) corresponding to the different palaeogeographic province of the Tethyan realm. The palaeocurrent pattern of the Gurnigel nappe indicates a northern direction which is deflected eastward along the oceanic trench (Caron et al., 1980; Winkler, 1984; Wildi, 1985) (Fig. 24). Both the palaeocurrent pattern and biostratigraphy further suggest a westward migration of the detrital source linked to the scissor closure of the basin (Winkler, 1984). Moreover, biostratigraphic work by (Ujetz, 1996) and, more recently, (Ospina-Ostios et al., 2013) showed that the sedimentation of this flysch took place in a time interval between the Middle Eocene and the Late Eocene/Early Oligocene. In this period, the sedimentary accretionary prism comprised the Briançonnais and Piemont sedimentary covers (Mosar et al., 1996, Fig. 7) and, in the highest position, of the Sesia-Dent Blanche nappe (Schmid et al., 1996; Handy et al., 2010) (Fig. 25). The latter of which was partially obducted and formed the back stop of the Alpine Tethys accretionary prism (Stampfli et al., 1998; Manzotti et al., 2014). This prism was separated from the Southern Alps by the Periadriatic fault. Hence, no sediments from the Southern Alps could contribute to flysch deposition in the Alpine Tethys, except for those already reworked during the initiation of subduction (e.g. the Simme Flysch) explaining how Southern Alps-derived volcanic grains of Triassic age (205 Ma peak, Fig. 23) occur in the Gurnigel nappe (Bütler et al., 2011) and Médianes Flysch (Beltrán-Triviño et al., 2013). In addition, the detrital zircon population pertaining to 468-425 Ma peak can also be related to the Southern Alps.

The Sesia-Dent Blanche nappe is composed of an igneous basement and of sedimentary covers metamorphosed during the Late Cretaceous (Manzotti et al., 2014). It formed the metamorphic belt of the Tethyan accretionary prism (Figs. 23 and 24). The geochemistry of garnets from the Voirons Flysch suggests derivation from metasedimentary rocks and (metamorphosed?) igneous rocks of similar composition to those described from the Sesia Dent-Blanche nappe (Fig. 22). Alm-Prp-Grs and Grs-And grains are indeed reported in metapelite; metabasite and calcsilicate rocks respectively from this unit (Dal Piaz et al., 1983). The former may also derive from recycled kinzigite preserved in the Eclogitic Micaschists Complex. A potential clinopyroxene-rich amphibolite from the Valpelline serie is also envisaged considering the metabasite source. Our data is in agreement with the garnet geochemical data of KIRST (2014) from metasedimentary rocks of the Becca d'Aver continental sliver. Almandine-rich garnet is also reported in the Lombardian Flysch of the Southern Alps (Bernoulli and Winkler, 1990) corroborating that the Sesia Dent-Blanche nappe could be the source of garnets. Despite tourmaline being widespread in the Alps, geochemical data are scarce, preventing constraints on their origin. Finally, the few geochronological data (Manzotti et al., 2014 and Fig. 23) obtained from the Sesia-Dent

Blanche nappe could correspond to the 468–425 Ma range reported by Bütlér et al. (2011).

Rare andesite lithoclasts observed in the Voirons Sandstone Fm. (Ospina-Ostios et al., 2013, Fig. 4) cannot originate from the Sesia Dent-Blanche nappe due to the Oligocene age of the andesite layers from the external part of the Sesia-Lanzo unit (Venturelli et al., 1984, and references therein). Nevertheless, Upper Carboniferous–Permian volcanic deposits relating to the Variscan orogeny (Cortesogno et al., 1998) are a potential source of andesite grains. Volcanic Upper Carboniferous–Permian units are reported from (1) the Ligurian Alps and Sardinia in the Briançonnais domain (Cortesogno et al., 1998; Decarlis et al., 2013) and the Siviez-Mischabel nappe (Sartori et al., 2006), and (2) the Southern Alps (Cortesogno et al., 1998) through the Simme nappe. Most of this event may have been poorly preserved in detrital zircon or poorly contribute to the detrital sedimentation. Hence, the 310–260 Ma interval constitutes secondary peak and rarely high frequency peak (Bütlér et al., 2011, see sample 11EB07 in 280–300 Ma range for the latter). However, the oldest component may represent or at least contribute to the 346–315 Ma population of the detrital zircon (Bütlér et al., 2011, Fig. 23). A derivation from a volcanic arc developed along the southern Tethyan margin during the subduction of the Piemont Ocean (Gasinski et al., 1997) is excluded on the basis of a lack of coeval ages in detrital zircon (Bütlér et al., 2011; Beltrán-Triviño et al., 2013), and bentonite layers (Winkler et al., 1985b, 1990) might derive from the British Paleogene Igneous Province (Koch et al., 2015).

Likewise, the black sandstones pebbles of Paleozoic age (Fig. 6b) reported from the Vouan Conglomerate Fm. likely indicate an input from the Briançonnais basement. Such pebbles possibly originate from the Palaeozoic rift basin of the Zone Houillère (Fabre, 1961). In addition, recent detrital zircon geochronological data from the Dora Maira massif and the Zone Houillère (Manzotti et al., 2016) constrain the magmatic events between 330–340 Ma which correspond to the 346–315 Ma peak (Fig. 23). Moreover, a similar almandine-rich garnet geochemistry is reported from the Briançonnais basement (Fig. 22). An Alm-Prp-Grs composition is reported from the Siviez-Mischabel nappe (Thélin et al., 1990) as well as Alm-Sps composition from the Zone Houillère (Bucher and Bousquet, 2007) and Pontis nappe (Giorgis et al., 1999). However, pyrope grains documented in the Dora Maira massif by (Schertl et al., 1991) are absent. The combination of data suggests that the Briançonnais basement during its subduction is a likely detrital source (Fig. 24). Nevertheless, distinguishing this detrital source from the Sesia Dent-Blanche nappe remains problematic and might be resolved using additional analysis such as garnet geochronology (Baxter and Scherer, 2013).

Finally, the older detrital zircon geochronological data are widespread distributed and hence cannot constrain the detrital source. The 510–490 Ma range (Fig. 23) is reported from the Briançonnais domain and the Austro-alpine Silvretta nappe (Schaltegger and Gebauer, 1999). The 610–550 Ma range (Fig. 23) is linked to the oldest meta-sediments in the Briançonnais, Austro-alpine and Southern Alps (Schaltegger and Gebauer, 1999). In addition, although they match with several peaks (610–550, 468–425 and 346–315 Ma, Fig. 23), zircon ages from the northern Tethyan margin are irrelevant since no southward palaeocurrent is described in the Gurnigel nappe.

The exhumed metamorphic lithologies of the Sesia-Dent Blanche nappe, and to a lesser extent of the Briançonnais basement, could likely represent the Basement uplift tectonic setting (Dickinson et al., 1985) or the Axial belt provenance (Garzanti et al., 2004, 2007, 2010) of the Feldspathic petrofacies (Fig. 9). This is in agreement with the feldspar dominated and garnet-rich detrital composition of modern fluvial sediments shed by the Dent Blanche nappe (Garzanti et al., 2010). The accretionary prism fed the flysch deposits with reworked detrital grains of various lithologies (calcareous to crystalline rocks) (Fig. 24). These reworked sediments were depleted in unstable grains which gave them a mature composition (Velbel, 1985). The resulting detrital composition reflects the Clastic wedge provenance of the Garzanti model (Garzanti et al., 2007) and the Transitional continental to Mixed tectonic setting (Dickinson, 1985) of the Quartzose petrofacies (Fig. 9).

This palaeogeographic model of the Voirons Flysch (Fig. 24) differs from the well-accepted model applied to the other flyschs from the Gurnigel nappe (Winkler, 1983, 1984; Caron et al., 1989). The latter considers a Maastrichtian to Lutetian age (Van Stuijvenberg, 1979; Van Stuijvenberg and Jan du Chêne, 1980; Winkler, 1983, 1984), and constrains the deposition of the Gurnigel flyschs in a Piemont Ocean characterised by a sedimentary accretionary prism that was smaller at that time than in the Middle Eocene to Late Eocene/Early Oligocene (Fig. 25). Based on the palaeogeographic reconstructions for the Early Cenozoic (Schmid et al., 1996; Handy et al., 2010), the suggested detrital sources for these flyschs are restricted to the Sesia Dent-Blanche nappe and the Upper Prealps nappes (Fig. 25). The dispute thus lies on the younger age obtained for the Voirons Flysch (Ujetz, 1996; Ospina-Ostios et al., 2013), which precludes deposition in the Piemont domain. Further biostratigraphic investigations are needed to clarify the palaeogeographic locations for the entire Gurnigel nappe. As long as the biostratigraphy of this nappe is not completely resolved, the relationship of the Voirons

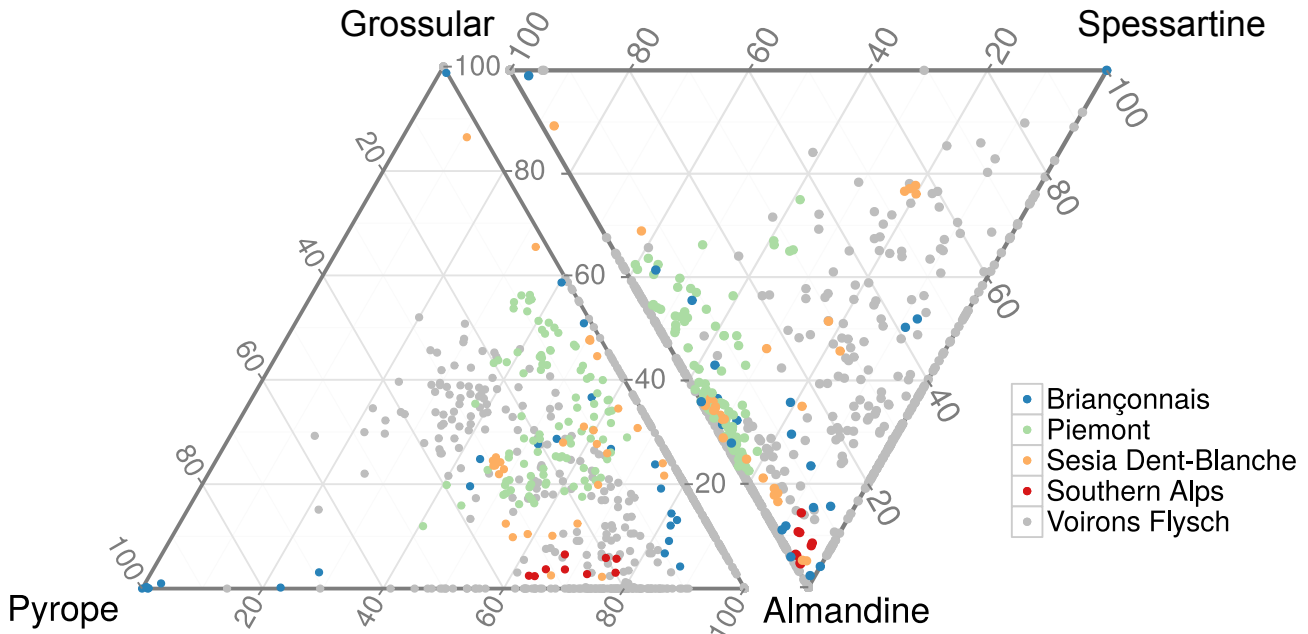


Figure 22: Major garnet end-member ternary diagram of middle to upper Penninic domains based on compilation of (Stutenbecker et al., 2016). Briançonnais: (Thélin et al., 1990), (Scherl et al., 1991), (Giorgis et al., 1999), (Bucher and Bousquet, 2007); Piemont: (Oberhansli, 1980), (Cartwright and Barnicoat, 2002), (Bucher and Grapes, 2009), (Weber and Bucher, 2015); Sesia–Dent Blanche: (Dal Piaz et al., 1983), (Gardien et al., 1994), (Kirst, 2014); Southern Alps: (Hunziker and Zingg, 1980)

Flysch with the rest of the Gurnigel nappe, and their respective palaeogeographic locations, remain a matter of debate.

6.6 Temporal evolution of the detrital inputs

The correlation of the petrofacies of the Voirons Flysch with the stratigraphy shows a temporal variation in the sediment supplies (Fig. 17a) as already suggested by (Winkler, 1984) for the rest of the Gurnigel nappe. Deposition began during the Middle Eocene with the Quartzose petrofacies in the Voirons Sandstone Fm. The source of the Feldspathic petrofacies was barely active at that time. In Late Eocene, inputs from the Feldspathic petrofacies markedly increased and alternated with those from the Quartzose petrofacies which progressively decreased. The fading of the Quartzose petrofacies concurred with the progradation of the turbiditic system and the deposition of the Vouan Conglomerate Fm. During these events, the source of the Quartzose petrofacies was either inactive or the detritus was shed to a different basin which remains unknown. The sharp contact between the Vouan Conglomerate Fm. and the Boëge Marl Fm. marks an abrupt modification both in the turbiditic system (development of a starved system) and in the sediment supply (the Quartzose petrofacies returns as the dominant supply) which may be related to major tectonic events. Finally, the gradual evolution towards the Bruant Sandstone Fm. indicates a steady-state system with an increase of sand-shale ratio dominated by the Quartzose petrofacies and sporadic inputs of the Feldspathic petrofacies.

7 Conclusions

Our study of the Voirons Flysch complements the existing dataset on the petrography of the flyschs from the Gurnigel nappe, and offers a new interpretation of the provenance of its constituent material.

1. In contrast to the other flysch units from the Gurnigel nappe, two distinctive sources have been identified in the Voirons Flysch,
 - The Quartzose petrofacies is the major detrital source. It is similar to the provenances described elsewhere in the Gurnigel nappe. It is a quartz-rich assemblage with sedimentary to magmatic

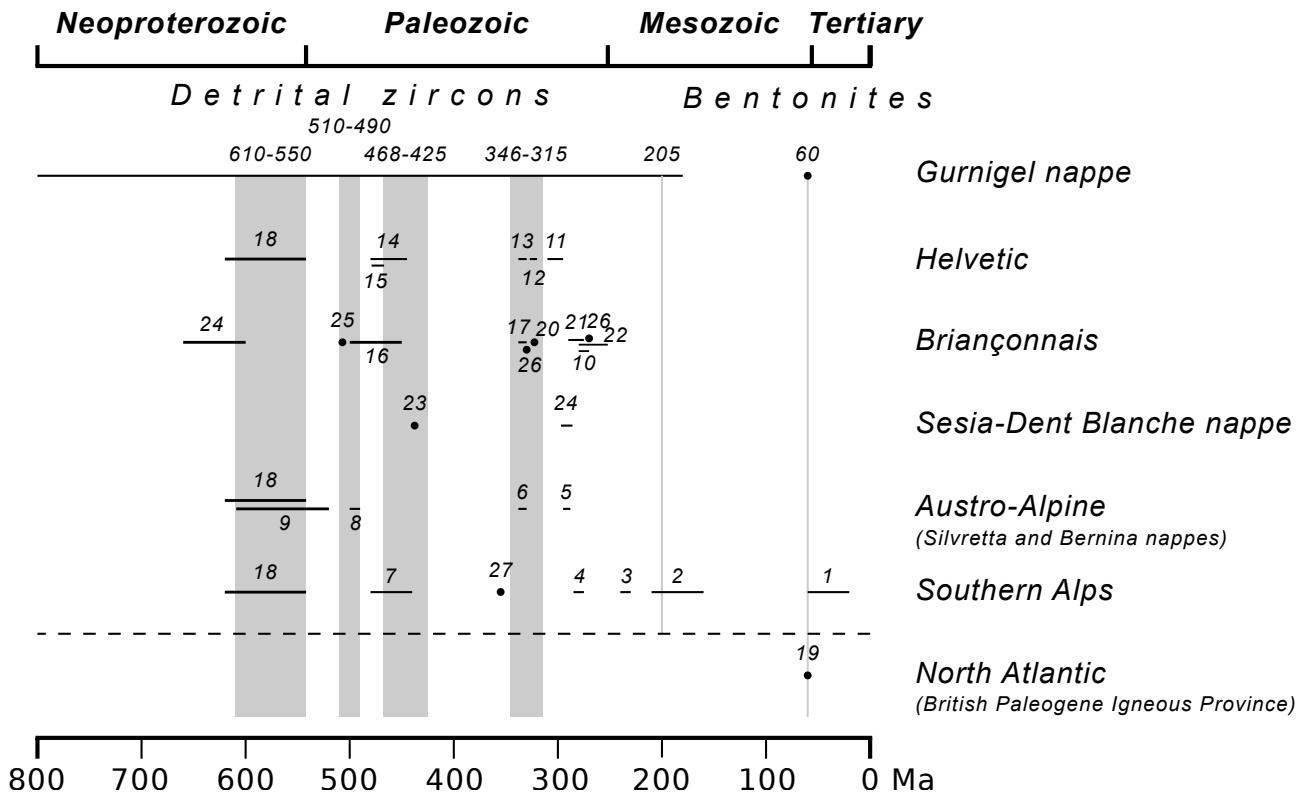


Figure 23: Major U/Pb age peaks of the detrital zircons (Bütler et al., 2011) and bentonites (Koch et al., 2015). Data are compared to the major magmatic events in the Tethyan realm based on the modified compilation of (Bütler et al., 2011). Bütler et al. (2011): 1–16; (Schaltegger and Gebauer, 1999): 18–24, 25; (Koch et al., 2015): 19; (Cortesogno et al., 1998): 20–22; (Manzotti et al., 2014): 23; (Bussy et al., 1996): 26

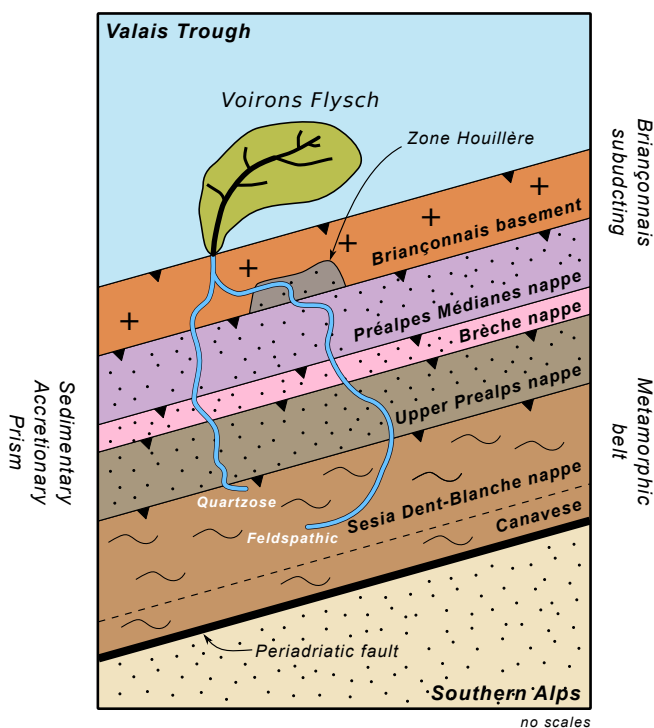


Figure 24: Palaeogeographic model of the Voirons Flysch and its two different detrital sources

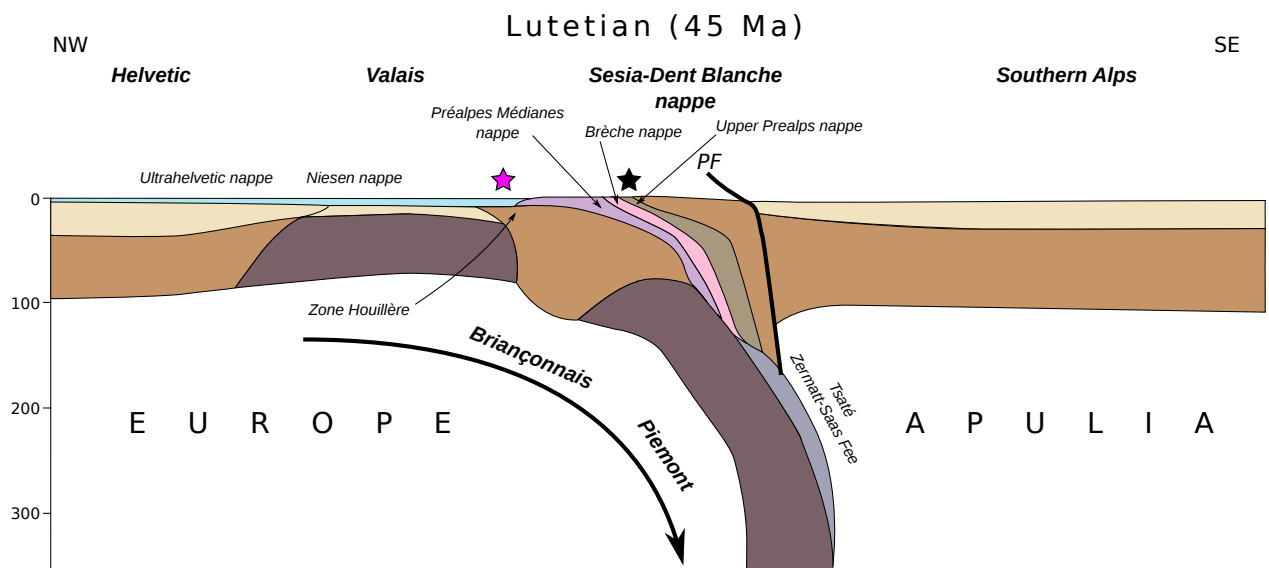


Figure 25: Cross section of the Tethyan realm during the Lutetian (Handy et al., 2010, modified). The stars indicate the paleogeographic location of the Voirons Flysch considering a Paleocene to Middle Eocene (black) and Middle to Late Eocene age (purple)

lithoclasts and a heavy-mineral assemblage dominated by ZTR + apatite. The most salient clasts in the conglomerate layers are pink granite fragments. The lithic composition variation reflects polycyclic sedimentary inputs corresponding to a Transitional continental block tectonic setting (Dickinson and Suczek, 1979) or a Clastic wedge provenance (Garzanti et al., 2007).

- The Feldspathic petrofacies represents a subordinate source in the Voirons Flysch, and has up to now not been identified elsewhere in the Gurnigel nappe. The Feldspathic petrofacies is mostly restricted to the Vouan Conglomerate Fm. Rock-fragment composition is characterised by black sandstones of Paleozoic age in conglomeratic layers. Garnet dominates the heavy-mineral assemblage, and metamorphic lithoclasts describe an Axial belt provenance (Garzanti et al., 2007) or a Basement uplift tectonic setting (Dickinson and Suczek, 1979) considering the feldspar-rich composition. Samples distribution shows punctual inputs of this secondary detrital source during deposition of the Quartzose petrofacies.
2. The random deposition of the Feldspathic petrofacies within lithologic units dominated by the Quartzose petrofacies, as well as the interfingering contact between the Voirons Sandstone Fm. and the Vouan Conglomerate Fm. confirm the stratigraphic nature of the contacts within the Voirons Flysch.
 3. A comparison of the Voirons Flysch with the Sarine and Dranses flyschs shows a similar quartz-rich composition, which indicates a similar source along the southern Tethyan margin and/or reworking of the latter deposits in the former.
 4. A palaeogeographic location of the Voirons Flysch in the Valais domain is suggested considering (1) the Middle Eocene to Late Eocene/Early Oligocene age obtained from planktonic foraminifera biostratigraphy (Ujetz, 1996 ; Ospina-Ostios et al., 2013), (2) the marked similarity of the black sandstone lithoclasts of Paleozoic age found in the Vouan Conglomerate Fm. with the Zone Houillère, (3) the resemblance of the Feldspathic petrofacies with the Médianes Flysch and (4) a potential Briançonnais source for the andesite rock-fragments.
 5. Our palaeogeographic model suggests that the Voirons Flysch was fed by the reworking of the sedimentary accretionary prism (Quartzose petrofacies) including the older Prealps nappes and by intermittent inputs from the Sesia Dent-Blanche nappe and possibly from the Briançonnais (Feldspathic petrofacies). However, identifying the detritus derived from the Briançonnais basement and that originating from the Sesia Dent-Blanche nappe is not straightforward. More accurate analysis (e.g. garnet geochronology) will be necessary to emphasise the detrital inputs from the Briançonnais units.

6. Our presented palaeogeographic model for the Voirons Flysch might eventually be applied to the other flyschs of the Gurnigel nappe if future biostratigraphic studies, possibly based on planktonic foraminifers, extend the Middle Eocene to Late Eocene/Early Oligocene age obtained for the Voirons Flysch to all deposits forming the Gurnigel nappe. Thus, further biostratigraphic investigations are urgently needed to clarify this palaeogeographic conundrum.

Acknowledgements

We thank François Gischig (University of Geneva) for technical help with thin sections and Dr. Mario Sartori (University of Geneva) for fruitful conversations. We are grateful to Franz Neubauer and an anonymous reviewer for constructive comments on an earlier manuscript.

Electronic supplementary materials

The online version of this article contains supplementary material:

- *Supplementary material 1*: Framework composition of the Voirons Flysch following the Gazzi-Dickinson method
- *Supplementary material 2*: SEM-EDS garnet geochemistry from the Voirons Flysch. Data include element and calculated oxide composition and enb-member abundance
- *Supplementary material 3*: SEM-EDS tourmaline geochemistry from the Voirons Flysch. Data include element and calculated oxide composition

References

- Ackermann, A. (1984). *Le Flysch de la nappe du Niesen*. PhD thesis, University of Fribourg.
- Ackermann, A. (1986). Le flysch de la nappe du Niesen. *Eclogae Geologicae Helvetiae*, 79(3):641–684, doi:10.5169/seals-165845.
- Ambrosetti, I. (2005). *Étude géologique de la région de la Valsainte (Préalpes fribourgeoises)*. PhD thesis, Fribourg University.
- Amorosi, A. and Zuffa, G. G. (2011). Sand composition changes across key boundaries of siliciclastic and hybrid depositional sequences. *Sedimentary Geology*, 236(1-2):153–163, doi:10.1016/j.sedgeo.2011.01.003.
- Argnani, A., Fontana, D., Stefani, C., and Zuffa, G. G. (2004). Late Cretaceous Carbonate Turbidites of the Northern Apennines: Shaking Adria at the Onset of Alpine Collision. *The Journal of Geology*, 112(2):251–259, doi:10.1086/381660.
- Arribas, J., Critelli, S., Le Pera, E., and Tortosa, A. (2000). Composition of modern stream sand derived from a mixture of sedimentary and metamorphic source rocks (Henares River, Central Spain). *Sedimentary Geology*, 133(1-2):27–48, doi:10.1016/S0037-0738(00)00026-9.
- Badoux, H. (1962). Géologie des Préalpes valaisannes. *Matériaux pour la Carte Géologique Suisse*, 113:86p.
- Badoux, H. (1965). Feuille et notice explicative de la feuille Thonon-Châtel (630) de la Carte géologique de la France (1/50000ème). BRGM, Orléans.
- Badoux, H. (1996). Le substratum des Préalpes du Chablais. *Bulletin de la Société vaudoise des Sciences Naturelles*, 84(2):113–124, doi:10.5169/seals-287992.
- Baker, G. (1962). Detrital heavy minerals in natural accumulate with special occurrence to australian occurrences. Technical Report Monograph series n°1, Australasian Institute of Mining and Metallurgy.
- Baxter, E. F. and Scherer, E. E. (2013). Garnet Geochronology: Timekeeper of Tectonometamorphic Processes. *Elements*, 9(6):433–438, doi:10.2113/gselements.9.6.433.
- Beltrán-Triviño, A., Winkler, W., and von Quadt, A. (2013). Tracing Alpine sediment sources through laser ablation U-Pb dating and Hf-isotopes of detrital zircons. *Sedimentology*, 60(1):197–224, doi:10.1111/sed.12006.

- Bernoulli, D. and Winkler, W. (1990). Heavy mineral assemblages from Upper Cretaceous South and Austroalpine flysch sequences (Northern Italy and Southern Switzerland): source terranes and palaeotectonic implications. *Eclogae Geologicae Helvetiae*, 83(2):287–310, doi:10.5169/seals-166588.
- Bertrand, J. and Delaloye, M. (1976). Datation par la méthode K-Ar de diverses ophiolites du flysch des Gets (Haute-Savoie, France). *Eclogae Geologicae Helvetiae*, 69(2):335–341, doi:10.5169/seals-164513.
- Bill, M., Bussy, F., Cosca, M. A., Masson, H., and Hunziker, J. C. (1997). High precision U-Pb and $^{40}\text{Ar}/^{39}\text{Ar}$ dating of an Alpine ophiolite (Gets nappe, French Alps). *Eclogae Geologicae Helvetiae*, 90(1):43–54, doi:10.5169/seals-168144.
- Bouma, A. H. (1962). *Sedimentology of Some Flysch Deposits: A Graphic Approach to Facies Interpretation*. Elsevier, Amsterdam.
- Broudoux, B. (1985). *Géologie des unités de Vanoise septentrionale et méridionale de Pralognan à Tignes (Alpes de Savoie)*. PhD thesis, Université des Sciences et Technologie de Lille 1.
- Brouwner, J. (1965). Agglutinated Foraminifera from some Turbiditic Sequences. *Proceedings of the Koninklijke Nederlandse Akademie van Wetenschappen, Series A*, 68(5):309–334.
- Bucher, K. and Grapes, R. (2009). The eclogite-facies Allalin gabbro of the Zermatt-Saas ophiolite, Western alps: A record of subduction zone hydration. *Journal of Petrology*, 50(8):1405–1442, doi:10.1093/petrology/egp035.
- Bucher, S. and Bousquet, R. (2007). Metamorphic evolution of the Briançonnais units along the ECORS-CROP profile (Western Alps): new data on metasedimentary rocks. *Swiss Journal of Geosciences*, 100(2):227–242, doi:10.1007/s00015-007-1222-4.
- Bussy, F., Sartori, M., and Thélin, P. (1996). U-Pb zircon dating in the middle Penninic basement of the Western Alps (Valais, Switzerland). *Schweizerische Mineralogische und Petrographische Mitteilungen*, 76(1):81–84, doi:10.5169/seals-57689.
- Bütler, E., Winkler, W., and Guillong, M. (2011). Laser ablation U/Pb age patterns of detrital zircons in the Schlieren Flysch (Central Switzerland): new evidence on the detrital sources. *Swiss Journal of Geosciences*, 104(2):225–236, doi:10.1007/s00015-011-0065-1.
- Caron, C. (1972). La Nappe Supérieure des Préalpes: subdivisions et principaux caractères du sommet de l'édifice préalpin. *Eclogae Geologicae Helvetiae*, 65(1):57–73, doi:10.5169/seals-164076.
- Caron, C. (1976). La nappe du Gurnigel dans les Préalpes. *Eclogae Geologicae Helvetiae*, 69(2):297–308, doi:10.5169/seals-164510.
- Caron, C., Homewood, P., Morel, R., and Van Stuijvenberg, J. (1980). Témoins de la Nappe du Gurnigel sur les Préalpes médianes: une confirmation de son origine ultrabriançonnaise. *Bulletin de la Société fribourgeoise des Sciences naturelles*, 69(1):64–79, doi:10.5169/seals-308586.
- Caron, C., Homewood, P., and Wildi, W. (1989). The original Swiss flysch: a reappraisal of the type deposits in the Swiss Prealps. *Earth-Science Reviews*, 26(1-3):1–45, doi:10.1016/0012-8252(89)90002-0.
- Cartwright, I. and Barnicoat, A. C. (2002). Petrology, geochronology, and tectonics of shear zones in the Zermatt-Saas and Combin zones of the Western Alps. *Journal of Metamorphic Geology*, 20(2):263–281, doi:10.1046/j.0263-4929.2001.00366.x.
- Charollais, J., Plancherel, R., Monjuvent, G., and Debeltas, J. (1998). *Notice explicative de la Carte géologique de la France (1/50000ème) - Feuille Annemasse (654)*. BRGM, Orléans.
- Cogulu, E. (1961). La géologie des Voirons et de la colline des Allinges. Master's thesis, University of Geneva.
- Copjaková, R., Sulovský, P., and Paterson, B. A. (2005). Major and trace elements in pyrope-almandine garnets as sediment provenance indicators of the Lower Carboniferous Culm sediments, Drahany Uplands, Bohemian Massif. *Lithos*, 82(1–2):51–70, doi:10.1016/j.lithos.2004.12.006.
- Coppo, N. (1999). Géologie de la région Voirons - Vouan. Master's thesis, University of Geneva.
- Cortesogno, L., Cassinis, G., Dallagiovanna, G., Gaggero, L., Oggiano, G., Ronchi, A., Seno, S., and Vanossi, M. (1998). The Variscan post-collisional volcanism in Late Carboniferous-Permian sequences of Ligurian Alps, Southern Alps and Sardinia (Italy): a synthesis. *Lithos*, 45(1-4):305–328, doi:10.1016/S0024-4937(98)00037-1.
- Crimes, P. T., Goldring, R., Homewood, P., van Stuijvenberg, J., and Winkler, W. (1981). Trace fossil assemblages of deep-sea fan deposits, Gurnigel and Schlieren flysch (Cretaceous-Eocene, Switzerland). *Eclogae Geologicae Helvetiae*, 74(3):953–995, doi:10.5169/seals-165136.
- Critelli, S., Le Pera, E., Galluzzo, F., Milli, S., Moscatelli, M., Perrotta, S., and Santantonio, M. (2007). Interpreting

- siliciclastic-carbonate detrital modes in foreland basin systems: An example from Upper Miocene arenites of the central Apennines, Italy. In Arribas, J., Critelli, S., and Johnsson, M. J., editors, *Sedimentary Provenance and Petrogenesis: Perspectives from Petrography and Geochemistry*, volume 420, chapter 8, pages 107–133. Geological Society of America, special pa edition.
- Dal Piaz, G. V., Lombardo, B., and Goso, G. (1983). Metamorphic evolution of the Mt. Emilius Klippe, Dent Blanche nappe, Western Alps. *American Journal of Science*, 283 A:438–458.
- Das Gupta, K. and Pickering, K. T. (2008). Petrography and temporal changes in petrofacies of deep-marine Ainsa-Jaca basin sandstone systems, Early and Middle Eocene, Spanish Pyrenees. *Sedimentology*, 55(4):1083–1114, doi:10.1111/j.1365-3091.2007.00937.x.
- de Kaenel, E., von Salis Perch-Nielsen, K., and Lindinger, M. (1989). The Cretaceous/Tertiary boundary in the Gurnigel Flysch (Switzerland). *Eclogae Geologicae Helvetiae*, 82(2):555–581, doi:10.5169/seals-166389.
- de Mortillet, G. (1863). Succin des Allinges. *Revue Savoisienne*, 1:7.
- Decarlis, A., Dallagiovanna, G., Lualdi, A., Maino, M., and Seno, S. (2013). Stratigraphic evolution in the Ligurian Alps between Variscan heritages and the Alpine Tethys opening: A review. *Earth-Science Reviews*, 125:43–68, doi:10.1016/j.earscirev.2013.07.001.
- Dickinson, W. R. A. (1985). Interpreting Provenance Relations from Detrital Modes of Sandstones. In Zuffa, G. G., editor, *Provenance of Arenites*, volume 148 of *NATO ASI - Series C: Mathematical and Physics Sciences*, chapter 15, pages 333–361. D. Reidel Publishing Compagny, Dordrecht, Holland.
- Dickinson, W. R. A., Beard, L. S., Brakenridge, G. R., Erjavec, J. L., Ferguson, R. C., Inman, K. F., Knepp, R. A., Lindberg, F. A., and Ryberg, P. T. (1983). Provenance of North American Phanerozoic sandstones in relation to tectonic setting. *Geological Society of America Bulletin*, 94(2):222, doi:10.1130/0016-7606(1983)94:222:PONAPS;2.0.CO;2.
- Dickinson, W. R. A. and Rich, E. I. (1972). Petrologic Intervals and Petrofacies in the Great Valley Sequence, Sacramento Valley, California. *Geological Society of America Bulletin*, 83(10):3007–3024, doi:10.1130/0016-7606(1972)83[3007:PIAPIT]2.0.CO;2.
- Dickinson, W. R. A. and Suczek, C. (1979). Plate Tectonics and Sandstone Compositions. *AAPG Bulletin*, 63(12):2164–2182, doi:10.1306/2F9188FB-16CE-11D7-8645000102C1865D.
- Egger, H., Homayoun, M., Huber, H., Rögl, F., and Schmitz, B. (2005). Early Eocene climatic, volcanic, and biotic events in the northwestern Tethyan Untersberg section, Austria. *Palaeogeography, Palaeoclimatology, Palaeoecology*, 217(3-4):243–264, doi:10.1016/j.palaeo.2004.12.006.
- Fabre, J. (1961). Contribution à l'étude de la Zone Houillère en Maurienne et en Tarentaise (Alpes de Savoie). *Mémoire du BRGM*, 2:1–315.
- Flück, W. (1973). Die Flysche der praealpinen Decken im Simmental und Saanenland. *Matériaux pour la Carte Géologique Suisse*, 146:87p.
- Follmi, K. B. (1990). Condensation and phosphogenesis: example of the Helvetic mid-Cretaceous (northern Tethyan margin). *Geological Society, London, Special Publications*, 52(1):237–252, doi:10.1144/GSL.SP.1990.052.01.17.
- Frébourg, G. (2006). *Les Conglomérats du Vouan: un cañon turbiditique?* PhD thesis, University of Geneva.
- Füchtbauer, H. (1964). Sedimentpetrographische Untersuchungen in der älteren Molasse nördlich der Alpen. *Eclogae Geologicae Helvetiae*, 57(1):11–298, doi:10.5169/seals-163140.
- Gagnebin, E. (1944). Présence du Barrémien ultra-hélvétique à St-Gingolph (Valais). *Eclogae Geologicae Helvetiae*, 37(2):195–197, doi:10.5169/seals-160499.
- Gardien, V., Reusser, E., and Marquer, D. (1994). Pre-Alpine metamorphic evolution of the gneisses from the Valpelline series (Western Alps, Italy). *Schweizerische Mineralogische und Petrographische Mitteilungen*, 74(3):489–502, doi:10.5169/seals-56364.
- Garzanti, E. (1991). Non-Carbonate Intrabasinal Grains in Arenites: Their Recognition, Significance, and Relationship to Eustatic Cycles and Tectonic Setting. *Journal of Sedimentary Research*, 61(6):959–975, doi:10.1306/D4267816-2B26-11D7-8648000102C1865D.
- Garzanti, E. and Andò, S. (2007). Plate tectonics and heavy-mineral suites of modern sands. In Mange, M. A. and Wright, D. T., editors, *Heavy minerals in use*, volume 58 of *Developments in Sedimentology*, chapter 34, pages 741–763. Elsevier, Amsterdam.

- Garzanti, E., Doglioni, C., Vezzoli, G., and Andò, S. (2007). Orogenic Belts and Orogenic Sediment Provenance. *The Journal of Geology*, 115(3):315–334, doi:10.1086/512755.
- Garzanti, E., Resentini, A., Vezzoli, G., Andò, S., Malusà, M. G., Padoan, M., and Paparella, P. (2010). Detrital Fingerprints of Fossil Continental-Subduction Zones (Axial Belt Provenance, European Alps). *The Journal of Geology*, 118(4):341–362, doi:10.1086/652720.
- Garzanti, E. and Vezzoli, G. (2003). A Classification of Metamorphic Grains in Sands Based on their Composition and Grade. *Journal of Sedimentary Research*, 73(5):830–837, doi:10.1306/012203730830.
- Garzanti, E., Vezzoli, G., Lombardo, B., Andò, S., Mauri, E., Monguzzi, S., and Russo, M. (2004). Collision-Orogen Provenance (Western Alps): Detrital Signatures and Unroofing Trends. *The Journal of Geology*, 112(2):145–164, doi:10.1086/381655.
- Gasinski, A., Slaczka, A., and Winkler, W. (1997). Tectono-sedimentary evolution of the Upper Prealpine nappe (Switzerland and France): nappe formation by Late Cretaceous-Paleogene accretion. *Geodinamica Acta*, 10(4):137–157, doi:10.1080/09853111.1997.11105299.
- Giorgis, D., Thelin, P., Stampfli, G. M., and Bussy, F. (1999). The Mont-Mort metapelites: Variscan metamorphism and geodynamic context (Briançonnais basement, Western Alps, Switzerland). *Schweizerische Mineralogische und Petrographische Mitteilungen*, 79(3):381–398, doi:10.5169/seals-60214.
- Gottlieb, P., Wilkie, G., Sutherland, D., Ho-Tun, E., Suthers, S., Perera, K., Jenkins, B., Spencer, S., Butcher, A., and Rayner, J. (2000). Using quantitative electron microscopy for process mineralogy applications. *JOM*, 52(4):24–25, doi:10.1007/s11837-000-0126-9.
- Grew, E. S., Locock, A. J., Mills, S. J., Galuskin, I. O., Galuskin, E. V., and Halenius, U. (2013). Nomenclature of the garnet supergroup. *American Mineralogist*, 98(4):785–811, doi:10.2138/am.2013.4201.
- Hamilton, N. (2016). ggtern: An Extension to 'ggplot2', for the Creation of Ternary Diagrams.
- Handy, M. R., M. Schmid, S., Bousquet, R., Kissling, E., and Bernoulli, D. (2010). Reconciling plate-tectonic reconstructions of Alpine Tethys with the geological-geophysical record of spreading and subduction in the Alps. *Earth-Science Reviews*, 102(3-4):121–158, doi:10.1016/j.earscirev.2010.06.002.
- Henry, D. J. and Guidotti, C. V. (1985). Tourmaline as a petrogenetic indicator mineral: an example from the staurolite-grade metapelites of NW Maine. *American Mineralogist*, 70(1-2):1–15.
- Hsü, J. K. (1960). Palaeocurrent structures and paleogeography of the Ultrahelvetic flysch basins, Switzerland. *Geological Society of America Bulletin*, 71(5):577–610, doi:10.1130/0016-7606(1960)71[577:PSAPOT]2.0.CO;2.
- Hsü, J. K. and Schlanger, S. O. (1971). Ultrahelvetic Flysch Sedimentation and Deformation Related to Plate Tectonics. *Geological Society of America Bulletin*, 82(5):1207–1217, doi:10.1130/0016-7606(1971)82[1207:UFSADR]2.0.CO;2.
- Hubert, J. F. (1967). Sedimentology Of Prealpine Flysch Sequences, Switzerland. *Journal of Sedimentary Research*, 37(3):885–907, doi:10.1306/74D717CB-2B21-11D7-8648000102C1865D.
- Hunziker, J. C. and Zingg, A. (1980). Lower Paleozoic Amphibolite to Granulite Facies Metamorphism im the Ivrea Zone (Southern Alps, Northern Italy). *Schweizerische Mineralogische und Petrographische Mitteilungen*, 60(2-3):181–213, doi:10.5169/seals-46667.
- Ingersoll, R. V. (1978). Petrofacies and Petrologic Evolution of the Late Cretaceous Fore-Arc Basin, Northern and Central California. *The Journal of Geology*, 86(3):335–352, doi:10.1086/649695.
- Ingersoll, R. V. (1990). Actualistic sandstone petrofacies: Discriminating modern and ancient source rocks. *Geology*, 18(8):733, doi:10.1130/0091-7613(1990)018:j.0733:ASPDMA;2.3.CO;2.
- Ingersoll, R. V., Ketchmer, A. G., and Valles, P. K. (1993). The effect of sampling scale on actualistic sandstone petrofacies. *Sedimentology*, 40(5):937–953, doi:10.1111/j.1365-3091.1993.tb01370.x.
- Ingersoll, R. V. and Suczek, C. (1979). Petrology and Provenance of Neogene Sand from Nicobar and Bengal Fans, DSDP Sites 211 and 218. *Journal of Sedimentary Research*, 49(4):1217–1228, doi:10.1306/212F78F1-2B24-11D7-8648000102C1865D.
- Jan du Chêne, R. (1977). Nouvelles données sur la palynostratigraphie des Flyschs des Préalpes externes (Suisse). *Archives des Sciences de la Société de Physique et d'Histoire naturelle de Genève*, 30(1):53–63.
- Jan du Chêne, R., Gorin, G., and van Stuijvenberg, J. (1975). Etude géologique et stratigraphique (palynologie et nannoflore calcaire) des Grès des Voirons (Paléogène de Haute-Savoie, France). *Géologie Alpine*, 51:51–78.
- Jeanbourquin, P., Kindler, P., and Dall'Agnolo, S. (1992). Les mélanges des Préalpes internes entre Arve et

- Rhône (Alpes occidentales franco-suisses). *Eclogae Geologicae Helvetiae*, 85(1):59–83, doi:10.5169/seals-166995.
- Kerrien, Y., Turrel, C., Monjuvent, G., Charollais, J., Lombard, A., Balmer, F., Olmari, F., Papillon, R., Fontannaz, L., Amberger, G., Ruchat, C., Grebert, Y., and Marthaler, M. (1998). Feuille Annemasse (654) de la Carte géologique de la France (1/50000ème).
- Kirst, F. (2014). *Progressive orogenic deformation and metamorphism along the Combin Fault and Dent Blanche Basal Thrust in the Swiss-Italian Western Alps*. Phd thesis, University of Bonn.
- Koch, S., Winkler, W., Von Quadt, A., and Ulmer, P. (2015). Paleocene and Early Eocene volcanic ash layers in the Schlieren Flysch, Switzerland: U–Pb dating and Hf-isotopes of zircons, pumice geochemistry and origin. *Lithos*, 236–237:324–337, doi:10.1016/j.lithos.2015.07.008.
- Krippner, A., Meinhold, G., Morton, A. C., and von Eynatten, H. (2014). Evaluation of garnet discrimination diagrams using geochemical data of garnets derived from various host rocks. *Sedimentary Geology*, 306:36–52, doi:10.1016/j.sedgeo.2014.03.004.
- Kuenen, P. H. and Carozzi, A. V. (1953). Turbidity Currents and Sliding in Geosynclinal Basins of the Alps. *The Journal of Geology*, 61(4):363–373, doi:10.1086/626101.
- Kuhn, J. A. (1972). Stratigraphisch-mikropaläontologische Untersuchungen in der Äusseren Einsiedler Schuppenzone und im Wägitaler Flysch E und W des Sihlsees (Kt. Schwyz). *Eclogae Geologicae Helvetiae*, 65(3):485–533, doi:10.5169/seals-164104.
- Lihou, J. C. and Mange-Rajetzky, M. A. (1996). Provenance of the Sardona Flysch, eastern Swiss Alps: example of high-resolution heavy mineral analysis applied to an ultrastable assemblage. *Sedimentary Geology*, 105(3–4):141–157, doi:10.1016/0037-0738(95)00147-6.
- Lombard, A. (1940). Géologie des Voirons. *Mémoire de la Société helvétique des Sciences Naturelles*, 74:118p.
- Mack, G. H. (1984). Exceptions to the Relationship Between Plate Tectonics and Sandstone Composition. *Journal of Sedimentary Research*, 54(1):212–220, doi:10.1306/212F83E6-2B24-11D7-8648000102C1865D.
- Mange, M. A. and Maurer, H. F. W. (1992). *Heavy Minerals in Colour*. Mange, Maria A. and Maurer, Heinz F. W.
- Mange, M. A. and Morton, A. C. (2007). Geochemistry of Heavy Minerals. In Mange, M. A. and Wright, D. T., editors, *Heavy Minerals in Use*, volume 58 of *Developments in Sedimentology*, chapter 13, pages 345–391. Elsevier, Amsterdam.
- Manzotti, P., Ballèvre, M., and Poujol, M. (2016). Detrital zircon geochronology in the Dora-Maira and Zone Houillère: a record of sediment travel paths in the Carboniferous. *Terra Nova*, 28(4):279–288, doi:10.1111/ter.12219.
- Manzotti, P., Ballèvre, M., Zucali, M., Robyr, M., and Engi, M. (2014). The tectonometamorphic evolution of the Sesia–Dent Blanche nappes (internal Western Alps): review and synthesis. *Swiss Journal of Geosciences*, 107(2–3):309–336, doi:10.1007/s00015-014-0172-x.
- Morad, S., Bergan, M., Knarud, R., and Nystuen, J. P. (1990). Albitization of Detrital Plagioclase in Triassic Reservoir Sandstones from the Snorre Field, Norwegian North Sea. *Journal of Sedimentary Research*, 60(3):411–425, doi:10.1306/212F91AB-2B24-11D7-8648000102C1865D.
- Morad, S., Kutzer, J. M., and De Ros, L. F. (2000). Spatial and temporal distribution of diagenetic alterations in siliciclastic rocks: implications for mass transfer in sedimentary basins. *Sedimentology*, 47:95–120, doi:10.1046/j.1365-3091.2000.00007.x.
- Morel, R. (1980). *Géologie du massif du Niremont (Préalpes romandes) et de ses abords*. PhD thesis, Université de Fribourg.
- Morton, A. C. and Hallsworth, C. R. (1994). Identifying provenance-specific features of detrital heavy mineral assemblages in sandstones. *Sedimentary Geology*, 90(3–4):241–256, doi:10.1016/0037-0738(94)90041-8.
- Morton, A. C. and Hallsworth, C. R. (1999). Processes controlling the composition of heavy mineral assemblages in sandstones. *Sedimentary Geology*, 124(1–4):3–29, doi:10.1016/S0037-0738(98)00118-3.
- Mosar, J. (1991). Géologie structurale dans les Préalpes Médianes (Suisse). *Eclogae Geologicae Helvetiae*, 84(3):689–725, doi:10.5169/seals-166793.
- Norman, M. B. (1974). Improved techniques for selective staining of feldspar and other minerals using amaranth. *Journal Research of the U.S. Geological Survey*, 2(2):73–79.
- Notholt, A. J. G., Sheldon, R. P., and Davidson, D. F. (1989). *Phosphate Deposits of the World. Volume 2. Phosphate Rock Resources*. Cambridge University Press, Cambridge.

- Oberhänsli, R. (1980). PT Bestimmungen anhand von Mineralanalysen in Eklogiten und Glaukophaniten der Ophiolite von Zermatt. *Bulletin suisse de minéralogie et pétrographie*, 60(2-3):215–235, doi:10.5169/seals-46668.
- Odin, G. S. and Matter, A. (1981). De glauconiarum origine. *Sedimentology*, 28(5):611–641, doi:10.1111/j.1365-3091.1981.tb01925.x.
- Ospina-Ostios, L. M., Ragusa, J., Wernli, R., and Kindler, P. (2013). Planktonic foraminifer biostratigraphy as a tool in constraining the timing of flysch deposition: Gurnigel flysch, Voirons massif (Haute-Savoie, France). *Sedimentology*, 60:225–238, doi:10.1111/sed.12013.
- Picard, M. D. and McBride, E. F. (2007). Comparison of river and beach sand composition with source rocks, Dolomite Alps drainage basins, northeastern Italy. In Arribas, J., Critelli, S., and Johnsson, M. J., editors, *Sedimentary Provenance and Petrogenesis: Perspectives from Petrography and Geochemistry*, volume 420, chapter 1, pages 1–12. Geological Society of America Special Paper.
- Pilloud, J. (1936). Contribution à l'étude stratigraphique des Voirons. Préalpes externes, Haute-Savoie. *Archives des Sciences de la Société de Physique et d'Histoire naturelle de Genève*, 18:219–249.
- R Core Team (2015). *R: A Language and Environment for Statistical Computing*. R Foundation for Statistical Computing, Vienna, Austria.
- Ragusa, J. (2009). Études des populations de minéraux lourds dans les Flyschs des Voirons et les Grès de Samoëns. Master's thesis, University of Geneva (unpublished).
- Ragusa, J. (2015). *Pétrographie, stratigraphie et provenance du Flysch des Voirons (Nappe du Gurnigel, Haute-Savoie, France)*. PhD thesis, University of Geneva (unpublished).
- Renevier, E. (1893). Géologie des Préalpes de la Savoie. *Eclogae Geologicae Helvetiae*, 4(1):53–73, doi:10.5169/seals-154920.
- Rigassi, D. (1958). Foraminifères des "Grès des Voirons". *Archives des Sciences de la Société de Physique et d'Histoire naturelle de Genève*, 11(3):398–400.
- Sarasin, C. (1894). De l'origine des blocs exotiques du Flysch. *Archives des Sciences de la Société de Physique et d'Histoire naturelle de Genève*, 32:67–101.
- Sartori, M., Gouffon, Y., and Marthaler, M. (2006). Harmonisation et définition des unités lithostratigraphiques briançonnaises dans les nappes penniques du Valais. *Eclogae Geologicae Helvetiae*, 99(3):363–407, doi:10.1007/s00015-006-1200-2.
- Schaltegger, U. and Gebauer, D. (1999). Pre-Alpine geochronology of the Central, Western and Southern Alps. *Schweizerische Mineralogische und Petrographische Mitteilungen*, 79(1):79–87, doi:10.5169/seals-60199.
- Schertl, H. P., Schreyer, W., and Chopin, C. (1991). The pyrope-coesite rocks and their country rocks at Parigi, Dora Maira Massif, Western Alps: detailed petrography, mineral chemistry and PT-path. *Contributions to Mineralogy and Petrology*, 108(1-2):1–21, doi:10.1007/BF00307322.
- Schmid, S. M., Fügenschuh, B., Kissling, E., and Schuster, R. (2004). Tectonic map and overall architecture of the Alpine orogen. *Eclogae Geologicae Helvetiae*, 97(1):93–117, doi:10.1007/s00015-004-1113-x.
- Schmid, S. M., Pfiffner, A. O., Froitzheim, N., Schönborn, G., and Kissling, E. (1996). Geophysical-geological transect and tectonic evolution of the Swiss-Italian Alps. *Tectonics*, 15(5):1036–1064, doi:10.1029/96TC00433.
- Stampfli, G. M. and Borel, G. D. (2002). A plate tectonic model for the Paleozoic and Mesozoic constrained by dynamic plate boundaries and restored synthetic oceanic isochrons. *Earth and Planetary Science Letters*, 196:17–33, doi:10.1016/S0012-821X(01)00588-X.
- Stampfli, G. M., Borel, G. D., Marchant, R., and Mosar, J. (2002). Western Alps geological constraints on western Tethyan reconstructions. In Rosenbaum, G. and Lister, G. S., editors, *Reconstruction of the evolution of the Alpine-Himalayan Orogen*, volume 7, pages 75–104. Journal of the Virtual Explorer.
- Stampfli, G. M., Mosar, J., Marquer, D., Marchant, R., Baudin, T., and Borel, G. D. (1998). Subduction and obduction processes in the Swiss Alps. *Tectonophysics*, 296(1-2):159–204, doi:10.1016/S0040-1951(98)00142-5.
- Stefani, C., Zattin, M., and Grandesso, P. (2007). Petrography of Paleogene turbiditic sedimentation in north-eastern Italy. In Arribas, J., Critelli, S., and Johnsson, M. J., editors, *Sedimentary Provenance and Petrogenesis: Perspectives from Petrography and Geochemistry*, volume 420, chapter 4, pages 37–55. Geological Society of America.
- Stutzenbecker, L., Berger, A., and Schlunegger, F. (2016). Detrital garnet fingerprint of the Central Swiss Alps. In *Swiss Geological Meeting*, page 177.

- SwissTopo (2008). Carte géologique et tectonique de la Suisse au 1:500'000.
- Tercier, J. (1928). Géologie de la Berra. *Matériaux pour la Carte Géologique Suisse*, 60:113 p.
- Thélin, P., Sartori, M., Lengeler, R., and Schaerer, J. P. (1990). Eclogites of Paleozoic or early Alpine age in the basement of the Penninic Siviez-Mischabel nappe, Wallis, Switzerland. *Lithos*, 25(1-3):71–88, doi:10.1016/0024-4937(90)90007-N.
- Trautwein, B., Dunkl, I., and Frisch, W. (2001). Accretionary history of the Rhenodanubian flysch zone in the Eastern Alps – evidence from apatite fission-track geochronology. *International Journal of Earth Sciences*, 90(3):703–713, doi:10.1007/s005310000184.
- Trümpy, R. (1960). Paleotectonic evolution of the central and western Alps. *Geological Society of America Bulletin*, 71(6):843–908, doi:10.1130/0016-7606(1960)71[843:PEOTCA]2.0.CO;2.
- Trümpy, R. (2006). Geologie der Iberger Klippen und ihrer Flysch-Unterlage. *Eclogae Geologicae Helvetiae*, 99(1):79–121, doi:10.5169/seals-169227.
- Ujetz, B. (1996). *Micropaleontology of Paleogene deep water sediments, Haute-Savoie, France*. PhD thesis, University of Geneva.
- Van der Plas, L. (1962). Preliminary note on the granulometric analysis of sedimentary rocks. *Sedimentology*, 1(2):145–157, doi:10.1111/j.1365-3091.1962.tb00031.x.
- Van Stuijvenberg, J. (1979). Geology of the Gurnigel area (Prealps, Switzerland). *Matériaux pour la Carte Géologique Suisse*, 151:111p.
- Van Stuijvenberg, J. (1980). Stratigraphie et structure de la Nappe du Gurnigel aux Voirons, Haute-Savoie. *Bulletin de la Société fribourgeoise des Sciences naturelles*, 69(1):80–96, doi:10.5169/seals-308587.
- Van Stuijvenberg, J. and Jan du Chêne, R. (1980). Nouvelles observations stratigraphiques dans le massif des Voirons. *Bulletin du BRGM*, 1(1):3–9.
- Van Stuijvenberg, J., Morel, R., and Jan du Chêne, R. (1976). Contribution à l'étude des flyschs de la région de Fayaux (Préalpes externes vaudoises). *Eclogae Geologicae Helvetiae*, 69(2):309–326, doi:10.5169/seals-164511.
- Velbel, M. A. (1985). Mineralogically Mature Sandstones in Accretionary Prisms. *Journal of Sedimentary Research*, 55(5):685–690, doi:10.1306/212F87BA-2B24-11D7-8648000102C1865D.
- Venturelli, G., Thorpe, R. S., Dal Piaz, G. V., Del Moro, A., and Potts, P. J. (1984). Petrogenesis of calc-alkaline, shoshonitic and associated ultrapotassic Oligocene volcanic rocks from the Northwestern Alps, Italy. *Contributions to Mineralogy and Petrology*, 86(3):209–220, doi:10.1007/BF00373666.
- Vial, R., Conrad, M. A., and Charollais, J. (1989). *Notice explicative de la feuille Douvaine (629) de la Carte géologique de la France (1/50000ème)*. BRGM, Orléans.
- von Eynatten, H. and Dunkl, I. (2012). Assessing the sediment factory: The role of single grain analysis. *Earth-Science Reviews*, 115(1-2):97–120, doi:10.1016/j.earscirev.2012.08.001.
- von Eynatten, H. and Gaupp, R. (1999). Provenance of Cretaceous synorogenic sandstones in the Eastern Alps: constraints from framework petrography, heavy mineral analysis and mineral chemistry. *Sedimentary Geology*, 124(1-4):81–111, doi:10.1016/S0037-0738(98)00122-5.
- Weber, S. and Bucher, K. (2015). An eclogite-bearing continental tectonic slice in the Zermatt–Saas high-pressure ophiolites at Trockener Steg (Zermatt, Swiss Western Alps). *Lithos*, 232:336–359, doi:10.1016/j.lithos.2015.07.010.
- Weidmann, M. (1967). Petite contribution à la connaissance du flysch. *Bulletin des Laboratoires de Géologie de l'Université de Lausanne*, 166:1–6.
- Weidmann, M. (1985). Géologie des Pléiades. *Bulletin de la Société vaudoise des Sciences Naturelles*, 77(367):195–204, doi:10.5169/seals-278511.
- Weidmann, M., Morel, R., and Van Stuijvenberg, J. (1976). La nappe du Gurnigel entre la Baye de Clarens et la Veveyse de Châtel. *Bulletin de la Société fribourgeoise des Sciences naturelles*, 65(3):182–196, doi:10.5169/seals-308540.
- Weltje, G. J. (2002). Quantitative analysis of detrital modes: statistically rigorous confidence regions in ternary diagrams and their use in sedimentary petrology. *Earth-Science Reviews*, 57(3-4):211–253, doi:10.1016/S0012-8252(01)00076-9.
- Whitney, D. L. and Evans, B. W. (2010). Abbreviations for names of rock-forming minerals. *American Mineralogist*, 95(1):185–187, doi:10.2138/am.2010.3371.

- Wildi, W. (1985). Heavy mineral distribution and dispersal pattern in penninic and ligurian flysch basins (Alps, northern Apennines). *Giornale di Geologia*, 47(1-2):77–99.
- Win, K. S., Takeuchi, M., Iwakiri, S., and Tokiwa, T. (2007). Provenance of detrital garnets from the Yukawa Formation, Yanase district, Shimanto belt, Kii Peninsula, Southwest Japan. *The Journal of the Geological Society of Japan*, 113(4):133–145, doi:10.5575/geosoc.113.133.
- Winkler, W. (1983). Stratigraphie, Sedimentologie und Sediment-petrographie des Schlieren-Flysches (Zentralschweiz). *Mériaux pour la Carte Géologique Suisse*, 158:115p.
- Winkler, W. (1984). Palaeocurrents and petrography of the Gurnigel-Schlieren flysch: A basin analysis. *Sedimentary Geology*, 40(1-3):169–189, doi:10.1016/0037-0738(84)90045-9.
- Winkler, W. (1993). Control factors on turbidite sedimentation in a deep-sea trench setting – The example of the Schlieren Flysch (Upper Maastrichtian-Lower Eocene, Central Switzerland). *Geodinamica Acta*, 6(2):81–102, doi:10.1080/09853111.1993.11105240.
- Winkler, W., Galetti, G., and Maggetti, M. (1985a). Bentonite im Gurnigel-, Schlieren- und Wägitäl Flysch: Mineralogie, Chemismus, Herkunft. *Eclogae Geologicae Helvetiae*, 78(3):545–564, doi:10.5169/seals-165670.
- Winkler, W., Hurford, A. J., von Salis Perch-Nielsen, K., and Odin, G. S. (1990). Fission track and nannofossil ages from a Palaeocene bentonite in the Schlieren Flysch (Central Alps, Switzerland). *Schweizerische mineralogische und petrographische Mitteilungen*, 70(3):389–396, doi:10.5169/seals-53629.
- Winkler, W., Wildi, W., Van Stuijvenberg, J., and Caron, C. (1985b). Wägitäl-Flysch et autres flyschs pennique en Suisse Centrale. Stratigraphie, sédimentologie et comparaisons. *Eclogae Geologicae Helvetiae*, 78(1):1–22, doi:10.5169/seals-165641.
- Wissing, S. B. and Pfiffner, A. O. (2002). Structure of the eastern Klippen nappe (BE, FR) : implications for its Alpine tectonic evolution. *Eclogae Geologicae Helvetiae*, 95(3):381–398, doi:10.5169/seals-168966.
- Young, S. W. (1976). Petrographic Textures of Detrital Polycrystalline Quartz as an Aid to Interpreting Crystalline Source Rocks. *Journal of Sedimentary Research*, 46(3):595–603, doi:10.1306/212F6FFA-2B24-11D7-8648000102C1865D.
- Zuffa, G. G. (1980). Hybrid Arenites: Their Composition and Classification. *Journal of Sedimentary Research*, 50(1):21–29, doi:10.1306/212F7950-2B24-11D7-8648000102C1865D.